Individual wave overtopping at coastal structures
A critical review and the existing challenges

Koosheh, Ali; Etemad-Shahidi, Amir; Cartwright, Nick; Tomlinson, Rodger; van Gent, Marcel R.A.

DOI
10.1016/j.apor.2020.102476

Publication date
2021

Document Version
Accepted author manuscript

Published in
Applied Ocean Research

Citation (APA)
Koosheh, A., Etemad-Shahidi, A., Cartwright, N., Tomlinson, R., & van Gent, M. R. A. (2021). Individual wave overtopping at coastal structures: A critical review and the existing challenges. *Applied Ocean Research*, *106*, 1-15. Article 102476. https://doi.org/10.1016/j.apor.2020.102476

Individual wave overtopping at coastal structures: A critical review and the existing challenges

Ali Koosheh [a], Amir Etemad-Shahidi [a, b *], Nick Cartwright [a], Rodger Tomlinson [c], Marcel R. A. van Gent [d, e]

[a] School of Engineering and Built Environment, Griffith University, Southport, QLD, 4222, Australia

[b] School of Engineering, Edith Cowan University, WA, 6027, Australia

[c] Griffith Centre for Coastal Management, Griffith University, Southport, QLD, 4222, Australia

[d] Department of Coastal Structures & Waves, Deltares, Delft, the Netherlands

[e] Department of Hydraulic Engineering, TU Delft, Delft, the Netherlands

* Corresponding author: a.etemadshahidi@griffith.edu.au

Abstract

Conventionally, allowable mean overtopping discharge is used as a design criterion for coastal structures. The mean overtopping discharge needs to be limited to ensure structural stability as well as the safety of people, vehicles, and properties behind the structure. Nowadays, limits for the maximum individual overtopping volumes are also specified in the design manuals, which requires the study of wave overtopping in wave-by-wave form. In some cases, in order to achieve more reliable safety for pedestrians and vehicles or to assess the stability of the inner slope, the maximum velocity and thickness of the overtopping flow need to be considered as well. The present paper aims to review the basic concepts of the individual wave overtopping such as the estimation of the probability of overtopping and the statistical methods to study the distribution of individual overtopping volumes. The temporal evolutions of the overtopping flow thickness / velocity along with the calculation of the overtopping discharge are discussed. Moreover, since the continuous recording of parameters is required for the study of individual wave overtopping, the most common experimental measurement and data analysis techniques with an emphasis on their advantages and limitations are discussed.

Keywords: wave overtopping; individual wave overtopping volume; probability of overtopping; overtopping flow thickness; overtopping flow velocity

1. Introduction

Due to continued population growth and the associated development of coastal areas, protection of people, infrastructures, and properties have become increasingly important concerns for coastal engineers and managers. In addition, climate change induced sea-level rise

and changing wave climate have increased the emphasis being placed on coastal protection structures. Accurate prediction of wave overtopping responses of these structures is a key factor for engineers in the creation of economical safe designs. Wave overtopping at coastal protection structures is a complex phenomenon influenced by many parameters such as the nearshore wave climate and the geometry and materials of the structure.

In order to estimate the extent of wave overtopping of these structures, many different overtopping parameters can be considered depending on the structure type and project's needs [1]. These include mean overtopping discharge, (q), individual maximum overtopping volume (V_{max}), overtopping flow velocity (u) and thickness (h) over the crest, as well as post-overtopping flow velocity / thickness on the leeward slope. With the exception of the mean overtopping discharge, all the other responses are parameters related to individual wave overtopping events and are obtained via '*wave-by-wave*' analysis. Since overtopping is a complex random process, analytical methods based on somewhat simplified expressions of the processes e. g.[2–4] do not necessarily always give reliable predictions [5]. Hence, estimations of overtopping parameters are mostly based on empirical methods relating overtopping response to wave and structural parameters. The existing empirical methods in overtopping manuals e. g.[1,6,7] are mostly derived from laboratory measurements using dimensional analysis and scaling arguments. The CLASH database [8] is one of the most comprehensive databases which includes datasets collected during the CLASH European project [9]. This database mostly focuses on average overtopping rates and very limited data related to wave-by-wave analysis are provided.

Historically, mean overtopping discharge has been considered the key parameter to describe the overtopping and it is generally used as the main criterion for the geometric design of structures. However, the results of experimental and field observations show that the maximum wave overtopping discharge during an overtopping event may be a thousand times larger than the mean overtopping discharge [10]. Therefore, the estimation of overtopping parameters associated with individual overtopping events is considered a critical factor for improved, safer design, see also [11–13]. In particular, waves with large volumes can be a serious threat for pedestrians or vehicles utilising the crest of the structure and for the inundation of infrastructure in the lee of the structure, even if the mean overtopping discharge is quite small. Hence, in recent design manuals e. g. [1], tolerable V_{max} values are specified for different structures and purposes such as structure stability, the safety of pedestrians, and vehicles. Lastly, the methods to estimate the maximum overtopping volume are only available for a limited number of structure types and are less well-validated [5].

Since individual wave overtopping events are random by nature, they should be described by their exceedance probability distribution which is then commonly related to the mean overtopping discharge (q), the probability of overtopping (P_{ow}) and the storm duration [14]. A two-parameter Weibull distribution has been suggested to describe the distribution of individual wave overtopping volumes and predict the maximum probable overtopping volume for sloping structures [10] and vertical walls [15]. In the case of protection of the leeward slope of dikes against erosion or the safety of people and vehicles, overtopping flow velocity and water layer thickness also become important. Their threshold values are examined for safe design, analogous to the criteria presented for human stability in river flood flows and urban drainage manuals e.g. [16–20].

Whilst the study of wave-by-wave overtopping has increased in recent years e.g. [21–23], gaps in knowledge exist in terms of the range of wave-structure parameter combinations that have been studied. Consequently, this paper provides a detailed review of publicly available studies on individual wave overtopping at sea defence structures with the aim of identifying current knowledge gaps to inform future studies. Although overtopping risk models may provide a high-level modelling e.g. [24,25], the present study is primarily dedicated to the review of measurement techniques and challenges, and risk modelling has been overviewed shortly. The paper is structured as follows: section 2 discusses the different aspects of individual wave overtopping volume including measurement techniques, probability distributions and the estimation of maximum overtopping volume. Section 3 focuses on the hydraulic parameters of overtopping flow namely velocity, thickness and discharge. Finally, the summary and discussions, and the main findings and recommendations for future studies are given in section 4.

2. Individual wave overtopping volume

2.1. Measurement techniques

All of the existing techniques for laboratory tests are based on the principle of measuring the temporal evolution of the overtopped water volume typically collected via a chute into a container behind the structure [26]. The volume in the container is then determined via measurement of either the water level or the mass. In general, there are two overtopping types, "(1) runs up the face of the structure and over the crest in coherent water mass (green water), (2) spray overtopping tends to occur when waves break seaward of the structure or break onto its seaward face (white water)"[1]. The second type may not contribute significantly to overtopping volumes especially when there is no significant wind velocity [1] . The water level in the container can be obtained using a surface piercing wave gauge e.g. [27,28] or a subsurface pressure transducer e.g. [29,30]. The main issues with this approach, are the water level fluctuations in the container due to the overtopping water effects. Possible solutions to filter out this unwanted 'noise' in the water level signal include: averaging the signal from multiple gauges spread throughout the container; installing a 'stilling' wall in the centre of the container which allows water to pass underneath thus reducing the oscillations behind the wall e.g. [31]. The alternative technique of determining the volume is by measuring the mass of overtopped water in the container using a weigh cell. The weigh cell can be positioned below the container [32] or the container may be suspended from the weigh cell [33]. In the case that the weigh cell is below the container, it is recommended that the container be kept in a dry area to eliminate the Archimedes force effect on the readings of the weigh cell. The accuracy of these types of measurements may differ, especially for small discharges. However, mean discharges less than 10^{-6} $m^3/s/m$ in small-scale experiments are commonly disregarded in the analysis since those discharges are negligible and possibly affected by scale-effects e.g. [34,35].

For measurements of significant discharges, the water level at the seaward side of the structure needs to be controlled in order to avoid that the still water level at the seaward side reduces. If

the water level in the wave flume decreases due to overtopping volumes or if the volume of the overtopping container is limited in comparison to the total volume of overtopping water, a pump can be installed preferably without any contact with the bottom of the container (see [36]). Using a pump can greatly increase the complexity of the experiment since its effect on the water level needs to be carefully accounted for in the recorded signals. For more details about the calibration of the pumping system and activating / deactivating the pump during the experiment, readers are referred to references [26,32,37].

Limited field measurements of wave overtopping especially in wave-by-wave form can be found in the literature. These kinds of studies may be quite different from small-scale studies in terms of both implemented instruments and measurement techniques. For the assessment of scale effects, the evaluation of the influence of measurement uncertainties and model effects [38] are also required to distinct the various sources of differences between prototype and model [39]. De Rouck et al. [40] investigated the scale effects on the measurement of wave overtopping discharge for different types of structures such as vertical walls [41] and rubble mound structures [30,42,43]. For vertical walls, they found good agreement between the prediction of overtopping at field and laboratory models where the negligible differences can be explained by model effects. However, a clear difference was observed for rubble mound structures, especially for the small overtopping values. This difference becomes more significant for longer and flatter slopes where scale model tests predict zero overtopping for an overtopped prototype situation. Regarding the measurement techniques, field studies are costly and complicated in terms of installation, maintenance, and monitoring. In situ measurements conventionally consist of a water tank at the crest or the lee side of the structure in which the water head is calculated using a pressure transducer e. g. [30,41,44,45]. Because of water level sloshing, spatially averaged measurement of water depths is needed. When measuring large overtopping volumes, the tank needs to be drained after reading an individual event. Estimating the maximum overtopping volume before the test is recommended to ensure that the tank will never overflow during the storm. Since the waves are often short-crested and the volume per wave varies considerably in time, overtopping events can vary along the structure [30]. Hence, the width of the tank (in the direction parallel to shoreline) should be large enough to have a representative calculation of discharge per metre of crest width. Recently, a new in-situ system based on a series of wires, WireWall [46], has been proposed to measure wave overtopping in the wave-by-wave form to provide site-specific calibration of overtopping tools and develop safety tolerances for flood risk management. This system is agile and easy to set up as no tank is needed to collect overtopping volumes. A series of capacitance wires are placed in the direction of wave attack to estimate different overtopping parameters such as the number of overtopping events, volume, flow thickness and velocity. In order to ensure the reliability and capability of this instrument for different field conditions, more studies and investigations are required to assess its advantages and disadvantages in comparison to the water tank system.

2.2 Overtopping event detection

The identification of an individual overtopping event based on the acquired data is another challenge in the wave-by-wave analysis. No robust technique is reported for the identification of the individual overtopping event. The existing techniques are mostly focused on innovative

solutions to improve the identification process. To identify individual overtopping events, different parameters such as overtopping flow thickness or discharge can be used. This depends on the case, instrumentation used, the goals of the study, and the required accuracy. Even if the occurrence of small events seems to be unimportant at the first sight, it should be noted that for the analysis of the probability of overtopping (P_{ow}), as well as the distribution of individual overtopping volumes (which lead to estimation of V_{max}), the number of overtopping events (N_{ow}) plays a significant role. These issues will be discussed more in the next sections.

One of the easiest ways of identifying overtopping is using individual wave volumes to derive the cumulative volume curve. This method was first adopted by Franco et al. [15] based on the assumption that each sudden increase in the volume shows the occurrence of an overtopping event. The recordings are usually noisy and hence a smooth curve is not easily obtained especially not if two subsequent events occur quickly after each other. In the case of large overtopping rates (e. g. low or negative crest freeboard structures) where the pumping system is needed due to the limited capacity of the container, the identification of individual overtopping events becomes more complicated. Extreme leaps and descending parts are observed in the cumulative volume curve and need to be accounted for in the analysis because of the pumping system and the large impact of water entering the container. Another challenge in the identification process is the delay between the occurrence of the overtopping event at the crest and the recorded signal in the container. Placing a wave gauge [47] or using two parallel strips of metal tape at the seaward edge of the crest [48] are some good examples of the identification systems. In these cases, the instruments (wave gauge or metal strips) are only used to detect the correct occurrence.

Fig. 1 shows the schematic time series of cumulative volume and the signal detected from the wave gauge at the structure crest. As can be seen, the recorded data from the detection system has a random nature and to obtain useful information, some interpretations are required. In order to identify the overtopping events automatically, “up / down crossing analysis” is usually applied by the definition of a constant threshold value. When the record exceeds (up-crosses) the threshold (green points), the overtopping begins and when it down-crosses (red points) the threshold, the overtopping ends (see Fig. 1). Hughes and Thornton [49] used an automatic up-crossing technique to identify overtopping events and controlled their results with manual observations (human supervised). However, the comparison of the results revealed that a considerable number of events were lost in the automatic identification system. This is because the automatic identification system was not able to identify all events (due to the signal complexity).

Some examples of the overtopping events which cannot be detected by the automatic identification system are discussed below. As seen in Fig. 1, a small event between t=204 s and t=205 s, cannot be detected because of having an amplitude lower than the threshold. The wave gauge signals between t=206 s and t=208 s, shows a large overtopping event. However, in this case, before the falling part of the signal reaches the threshold, another event begins, and the system cannot detect the occurrence of the new event. Hence, two subsequent overtopping events are considered as one. Also, two overtopping events are detected between t=209 s and t=210 s. Because the occurrence time of the mentioned events are close (in comparison to the signal pattern), it seems that they belong to one event. Obviously, the automatic up / down crossing method is sensitive to the threshold value and the selection of the

appropriate value of the threshold is somehow subjective and may need a trial and error process. As discussed in these examples, a low value of the threshold may merge a large overtopping event with the next events, while a high threshold value misses the small events. Platteeuw [50] proposed using the average of the five-hundredth lowest volume values as the identification threshold.

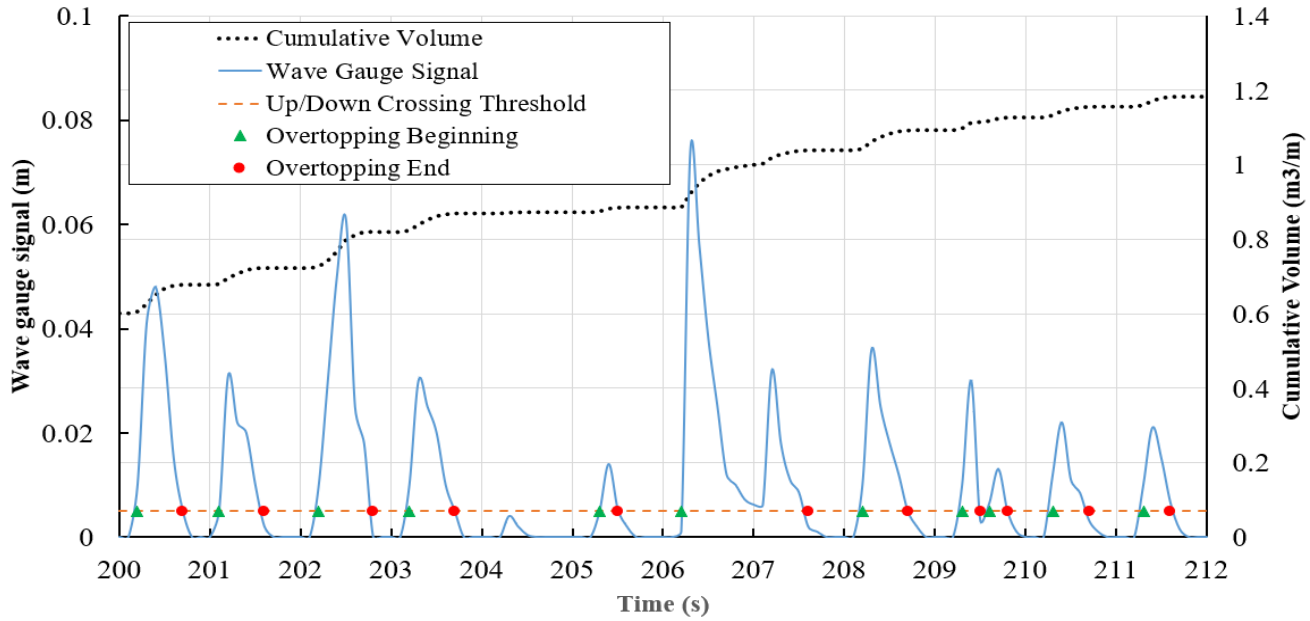

Fig. 1. Schematic overview of automatic overtopping identification using up / down crossing

Molines et al. [21] proposed an improved methodology for the automatic detection of the individual overtopping event. They defined q_1, the derivative of the volume as:

$$q_1(t_i) = \frac{V_0\left(t_i + \frac{T_m}{2}\right) - V_0(t_i)}{\frac{T_m}{2}} \quad (1)$$

where T_m is mean wave period. The following triangular moving average function was applied as a filter to eliminate frequencies higher than 3Hz (noise) in the derivative of volume:

$$q_2(t_i) = 0.25q_1(t_{i-1}) + 0.5q_1(t_i) + 0.25q_1(t_{i+1}) \quad (2)$$

Overtopping events were identified when the recorded volume is higher than a threshold, V_T. If a recorded overtopped volume is below the threshold, two scenarios may occur: (a) Some subsequent small overtopping events are detected with increasing time delay between their peak values. This shows that the detected values are the continuation of a large overtopping event and (b) There is a small local overtopping event with a higher value than those of surrounding small events which is a real small overtopping event. Finally, the overtopping events including those higher than the threshold and detected through the second scenario are re-analysed and the events closer than $0.8T_m$ are modified.

Formentin and Zanuttigh [23] also developed a semi-automatic procedure including two steps which is applicable for any recorded signal (e.g. overtopping flow thickness, discharge, …) from experimental or numerical tests. The first step is the wave identification based on the threshold up / down- crossing method where the lower threshold (l_{th}) and upper threshold (u_{th}) are defined. The implementation of the mentioned technique using two thresholds is schematically presented in Fig. 2(a). When the recorded signal down-crosses the lower threshold (l_{th}), an overtopping event is detected (hollow circles). The upper threshold (u_{th}) is always greater than the lower threshold (l_{th}) and eliminates the small oscillations in the signal which have the amplitude lower than thresholds differences (u_{th} - l_{th}). For example, the signal between t=205 s and t=206 s is discarded because it does not up-cross the higher threshold (u_{th}). On the other hand, some signals were discarded because they do not up-cross the lower threshold (l_{th}) (see the signal near the time = 210 s). The selection of the threshold values needs to be customized based on both structural and wave characteristics. For example, the difference of thresholds (u_{th} - l_{th}) depends on the incident significant wave height (H_s) and for emerged structures ($R_c > 0$) it should be lower than that of the submerged structures ($R_c < 0$).
The second step is the coupling system in which at least two wave gauges are required to be installed on the crest of the structure with a certain distance (d_w) in the direction of overtopping flow. An example of the coupled signals of two wave gauges is given in Fig. 2(b). First, the threshold up / down - crossing method is applied to both wave gauges as discussed. Then, for each detected wave at the first wave gauge, its corresponding pair must be found at the second wave gauge signal provided that the coupling criteria are satisfied. Since each coupling pairs from two wave gauges belong to a unique overtopping event that travels between the gauges, the time lag of their detection must be between dt_{min} and dt_{max}:

$$dt_{min} = max\left(\frac{d_w}{c_d}, \frac{1}{S_f}\right) \quad (3)$$

$$dt_{max} = \frac{d_w}{c_s} \quad (4)$$

where $c_d = L_{0,p} / T_p$ is the maximum wave celerity. Also, the sampling frequency (S_f), can affect the analysis and it is recommended to be more than c_d / d_w. The minimum possible celerity in shallow water (c_s) is computed based on the minimum value of the measured flow thickness at the first wave gauge (h_{1min}) as:

$$c_s = \sqrt{g h_{min}} \quad (5)$$

Any detected event that its corresponding pair is not found in the other gauge's signal or the found pair did not occur within [dt_{min}, dt_{max}] is discarded. For example, for the detected signals between t=202 s and t=203 s (first wave gauge) and between t=205 s and t=206 s (second wave gauge) in Fig. 2, no corresponding pair can be found in the other gauge. Also, two detected signals between t=211 s and t=212 s were discarded because their occurrence time delay is greater than dt_{max}. Another point that can be inferred from Fig. 2, is the lower amplitudes of recorded signals at the second wave gauge in comparison with those of the first wave gauge. This phenomenon can be observed in the structures with a permeable crest in

which a portion of overtopping water percolates into the structure body. Thus, some events may not be detected in the second wave gauge at all or discarded due to having an amplitude less than (u_{th} - l_{th}) in the up / down- crossing steps of the second wave gauge.

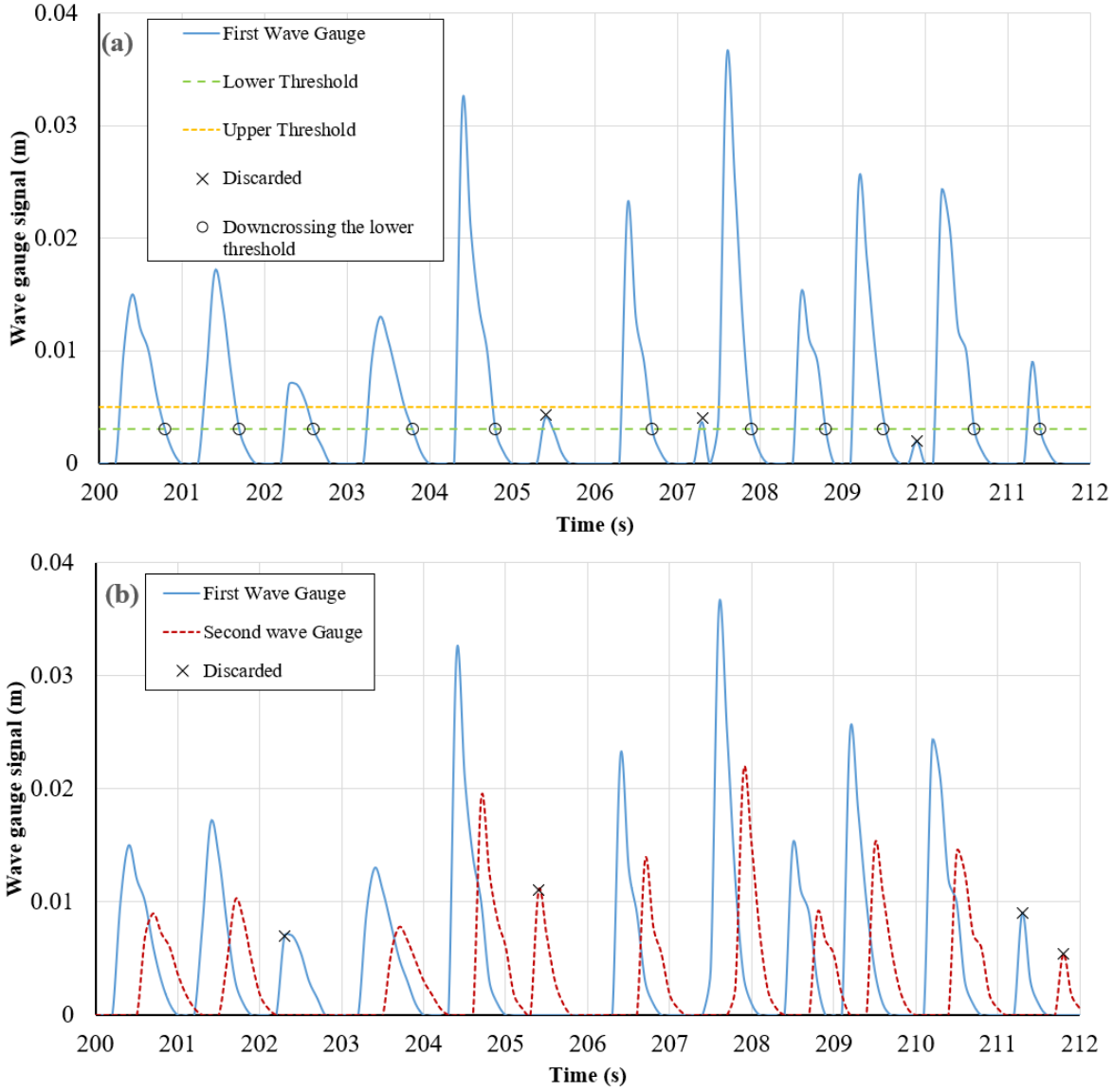

Fig.2. Semi-automatic detection of individual overtopping event, (a): threshold up / down- crossing method. (b): the coupling of two wave gauges signal (schematic)

2.3. Probability distribution

The simplest way to estimate the probability distribution of individual overtopping waves is by sorting overtopping volumes in descending order. The exceedance probability of each overtopping wave can be expressed as [51,52]:

$$\hat{P} = \frac{i}{N_{ow}+1} \quad (6)$$

where *i* is the rank of an individual wave volume and N_{ow} is the number of overtopping events. Van der Meer and Janssen [10] and Franco et al. [15] suggested the Weibull distribution to describe the probability distribution of individual overtopping volumes (*V*). Hence, the exceedance probability of each overtopping volume (P_v) can be estimated as:

$$P_v = \exp\left[-\left(\frac{V}{a}\right)^b\right] \quad (7)$$

The parameters *a* and *b* are known as the scale and shape factors of the Weibull distribution. The shape factor (*b*) as a non-dimensional parameter adjusts the extreme tail of the distribution, while the scale factor (*a*) as a dimensional scale normalizes the distribution [1]. According to the Weibull distribution, Van der Meer and Janssen [10] estimated the maximum individual overtopping volume based on the number of the overtopping waves (N_{ow}) as :

$$V_{max} = a\,[ln(N_{ow})]^{\frac{1}{b}} \quad (8)$$

A similar formula was later suggested by Lykke Andersen et al. [27] as:

$$V_{max} = a\,[ln(N_{ow}+1)]^{\frac{1}{b}} \quad (9)$$

Small value of *b* (e.g. *b* = 0.75) shows that overtopping events are mostly small and only a few large overtopping events may occur. Most of the structures with large crest freeboards follow this pattern of distribution. On the other hand, larger values of *b* (e. g. *b* = 3) mean that overtopping waves become significant and a more uniform distribution can be observed for the overtopping volumes [53]. This condition can be observed in the submerged structures such as levees where a layer of the overflow always exists on the structure crest.
By assuming the equality of measured mean overtopping volume ($\bar{V}_{meas}$) and the theoretical mean overtopping volume ($\bar{V}_{theor}$), Franco and Franco [14] derived the scale factor of Weibull distribution as:

$$a = \frac{1}{\Gamma(1+\frac{1}{b})}\frac{qN_wT_m}{N_{ow}} = \frac{1}{\Gamma(1+\frac{1}{b})}\frac{qT_m}{P_{ow}} \quad (10)$$

where Γ stands for the mathematical gamma function:

$$\Gamma(x) = \int_0^\infty t^{x-1}\,e^{-t}dt \quad (11)$$

The ratio of the number of overtopping waves (N_{ow}) to the number of incident waves (N_w), P_{ow} is known as the probability of overtopping. Eq. (10) shows that the scale factor (*a*) and the shape factor (*b*) are not independent of each other and the mean overtopping is a key parameter in the distribution of the individual overtopping volume. Victor [37] suggested a hyperbolic tangent fit for the coefficient $a' = \Gamma(1+\frac{1}{b})$:

$$a' = 1.13\tanh(1.32b) \quad (12)$$

The review of the early studies shows that the constant value of b = 0.75 was suggested for emergent structures such as sloped structures [10] and vertical walls [15]. Although the effect of wave steepness on the Weibull shape factor was considered in some studies (e.g. [47,54,55]) no definite relationship has been established between them. Victor et al. [56] pointed out that the influence of wave steepness on the shape factor is unclear and proposed the following formula for the shape factor:

$$b = exp\ (-2.0\ \frac{Rc}{H_{m0}}) + 0.15\cot\alpha + 0.56 \quad (13)$$

where R_c and H_{m0} stand for crest freeboard and significant wave height, respectively. Later, Gallach-Sánchez [26] proposed another similar formula which gives more accurate results than the method by Victor et al. [56]:

$$b = (0.59 + 0.23\cot\alpha)exp\ (-2.2\ \frac{Rc}{H_{m0}}) + 0.83 \quad (14)$$

There are also some other types of Weibull shape factor formulae e. g. [21,53,57] based on dimensionless mean overtopping discharge with the assumption that the effect of relative crest freeboard, slope angle and wave steepness exist implicitly in the mentioned parameter (see Appendix A). In the case of shallow water conditions in which the conventional formulae may give inferior results, Nørgaard et al. [58] suggested that:

$$b = \begin{cases} 0.75 & \frac{H_{m0}}{h_t} \leq 0.2 \quad \text{or} \quad H_{m0} / H_{\frac{1}{10}} \leq 0.848 \\ -6.1 + 8.08\frac{H_{m0}}{H_{\frac{1}{10}}} & \frac{H_{m0}}{h_t} > 0.2 \quad and \quad H_{m0} / H_{\frac{1}{10}} > 0.848 \end{cases} \quad (15)$$

where h_t is water depth at the toe of the structure and $H_{1/10}$ is the average of 1/10 highest incident waves, The Weibull analysis may not provide an accurate fit for the higher values of the volume. Therefore, some researchers preferred to use only the upper part of overtopping volumes to improve the Weibull fitting. There is however no consensus about the threshold value to be used for data selection. Unlike most of the previous studies, instead of the elimination of some data, Molines et al. [21] implemented the quadratic utility function in which all data is considered in the analysis in a weighted form. In this process, each overtopping volume (V_i) has the weight of $w_i = (V_i / V_{max})^2$ in the range of $0 < w_i \leq 1$.

The structures with negative crest freeboard such as levees and submerged dikes are subjected to combined wave overtopping and storm surge overflow. The average discharge (q_{ws}) can be written as the sum of the overtopping discharge (q_w) and the surge overflow discharge (q_s):

$$q_{ws} = q_w + q_s \quad (16)$$

Moreover, Eq. (10) is no longer valid and the Weibull parameters can be calculated through Eq. (A.7). Table 1 shows a summary of the proposed shape factors for different structures as

well as their characteristics. Fig. 3 compares different proposed shape factor equations. As seen, all given curves follow a similar pattern where for structures with $-1 \leq R_c/H_{m0} \leq 1$, a decreasing trend is observed. For the emerged structures with $R_c/H_{m0} > 1$, a constant value for shape factor can be adopted. For equations in which the effect of the slope is considered, curves are provided for both upper and lower limits of the range of applicability. Based on the proposed equations by Victor et al. [56] and Gallach-Sánchez [26] , it can be inferred that by increasing the slope (decrease of $cot\,\alpha$), the shape factor decreases. In Victor et al. [56] equation, the curves given for cot α = 2 and cot α = 0.36 diverge as R_c/H_{m0} increases. By contrast, the curves given by Gallach-Sánchez [26] converge as relative crest freeboard increase; implying that the effect of structure slope becomes less as R_c/H_{m0} increases. Hence, the effect of seaward slope variations on the Weibull shape factor needs to be investigated for different structure types, preferably within the same test set-up and using the same measurement and analysis techniques.

Most of studies in Table 1 (all except [15,59]) are based on (small-scale) 2D experiments representing head-on waves (as the worst condition for overtopping) and long-crested waves [58]. In the field, however, waves can be oblique and/or short-crested. If methods to account for the effects of oblique waves and short-crested waves that have been developed for overtopping discharges are adopted for other wave overtopping parameters, potential inaccuracies are introduced. The combination of wind waves from one direction and swell from another direction, can also be a challenge for estimating wave overtopping parameters such as the volume per overtopping wave. Researchers should also be aware of the changes that can occur due to wave interactions with the bathymetry, such as wave shoaling, wave refraction and wave breaking. Characteristics of incident waves should be measured at the toe of the structure. If not possible, incident waves at the toe position can be obtained from tests with the correct bathymetry but without the structure in position. Alternatively, numerical models can be calibrated and then used to transfer offshore wave to the toe of the structure e. g.[22].

With respect to the test programmes of wave overtopping studies, it is important that the key parameters (e. g. R_c / H_{m0}, $cot\,\alpha$) are within the practical ranges of these parameters, in order to provide relevant practical guidance.

Table 1: Summary of the studies of individual wave overtopping distribution

Reference	Shape factor (b)	Structure type	Relative crest freeboard	Slope angle	Portion of used upper data (%)
Van der Meer and Janssen [10]	0.75	Sloped – rough & smooth - impermeable	-	-	-
Franco et al. [15]	0.75	Vertical breakwater – smooth - permeable & impermeable	$0.8 \leq R_c \,/\, H_s \leq 2.8$ (Large-scale)	$cot\,\alpha = 0$	-
Besley [47]	Eqs. (A.1) and (A.2)	Vertical & Sloped	-	-	-
Bruce et al. [55]	0.74	Breakwater – rough - permeable	$0.8 \leq R_c \,/\, H_{m0} \leq 1.3$	$1.5 \leq cot\,\alpha \leq 2$	Greater than mean
Hughes and Nadal [60]	Eq. (A.3)	Levee - smooth - impermeable	$-2 \leq R_c \,/\, H_{m0} \leq -0.1$	$cot\,\alpha = 4.25$	10
Victor et al. [56]	Eq. (13)	Steep slopes - smooth - impermeable	$0.1 \leq R_c \,/\, H_{m0} \leq 1.69$	$0.36 \leq cot\,\alpha \leq 2.75$	50
Hughes et al. [61]	Eq. (A.4)	Sloped - rough & smooth - impermeable	$-2 \leq R_c \,/\, H_{m0} \leq 3.2$	$2.14 \leq cot\,\alpha \leq 4.25$	10
Zanuttigh et al. [53]	Eqs. (A.5) and (A.6)	Sloped - rough & smooth - permeable & impermeable	$-2 \leq R_c \,/\, H_{m0} \leq 3.2$	-	-
Nørgaard et al. [62]	Eq. (15)	Breakwater - rough - permeable	$0.9 \leq R_c \,/\, H_{m0} \leq 2$	$cot\,\alpha = 1.5$	30
Pan et al. [59]	Eq. (A.7)	Levee – Smooth - impermeable	$R_c \,/\, H_{m0} < 0$ (Large-scale)	$cot\,\alpha = 4.25$	100
Gallach-Sánchez [26]	Eq. (14)	Steep slopes and vertical – smooth & artificial rough - impermeable	$0 < R_c \,/\, H_{m0} \leq 3.25$	$0 \leq cot\,\alpha \leq 2$	10
Ju et al. [63]	Eq. (A.10)	Sloped – smooth – impermeable with berm	$0.5 < R_c \,/\, H_{m0} \leq 1.75$	$cot\,\alpha = 3$	100
Molines et al. [21]	Eq. (A.8)	Breakwater - rough - permeable	$1.2 < R_c \,/\, H_{m0} \leq 4.78$	$cot\,\alpha = 1.5$	100 (weighted)
Mares-Nasarre et al. [57]	Eq. (A.9)	Breakwater – rough - permeable	$0.33 < R_c \,/\, H_{m0} \leq 2.83$	$cot\,\alpha = 1.5$	100 (weighted)

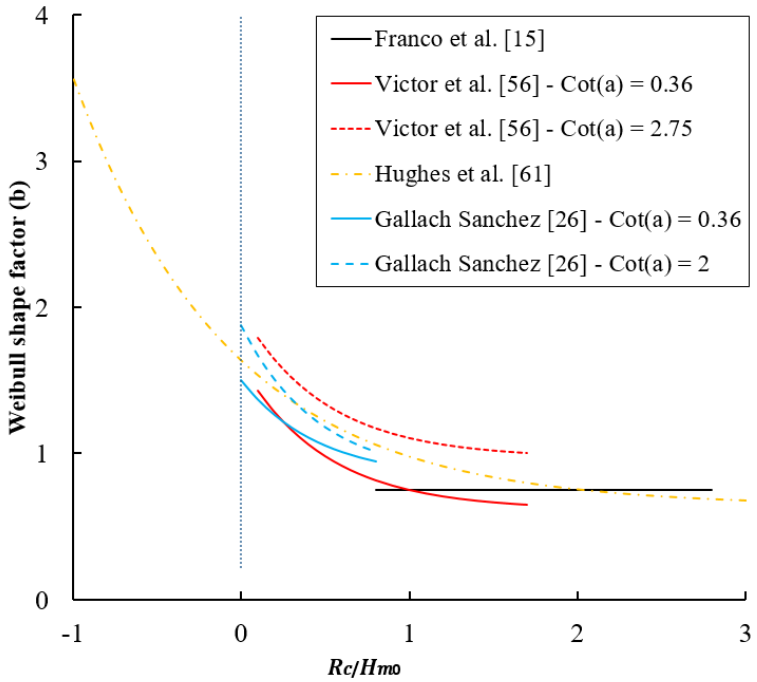

Fig. 3. Weibull shape function for different studies vs. relative crest freeboard

2.4. Probability of overtopping

The Weibull analysis of the individual wave overtopping volume and the estimation of the maximum individual overtopped volume rely on the number of the overtopping waves (N_{ow}). This quantity is usually expressed in the form of the probability of overtopping defined at the exposed structure:

$$P_{ow} = \frac{N_{ow}}{N_w} \tag{17}$$

where N_w is the number of incident waves. The estimation of the P_{ow} is challenging when very small overtopping events occur. The probability of overtopping is commonly related to relative crest freeboard (R_c/H_{m0}) as:

$$P_{ow} = exp\ (-(\frac{1}{\chi}\frac{R_c}{H_{m0}})^2) \tag{18}$$

The coefficient χ can be calculated as:

$$\chi = \frac{1}{\sqrt{-ln(0.02)}}\frac{R_{u2\%}}{H_{m0}} \tag{19}$$

$R_{u2\%}$ is the run-up height which is exceeded by 2% of incident waves at the toe of the structure. The estimation of $R_{u2\%}/H_{m0}$ needs to be calibrated for different structures under different wave conditions since many uncertainties exist and methods to predict $R_{u2\%}$ are simply not available, especially for complex structures.

Fig. 4 compares the proposed equations for the estimation of the overtopping probability (P_{ow}) as a function of relative crest freeboard (R_c/H_{m0})(Appendix B). In general, the overtopping probability values of sloped structures (e.g. Van der Meer and Janssen [10]; Victor et al. [56]) are higher than those of (deep water) vertical walls (e. g. Franco et al. [15]; theoretical curve) for a certain value of relative crest freeboard. By increasing R_c/H_{m0}, the vertical structures curve shows a very sharp decrease and the overtopping probability becomes zero for R_c/H_{m0} > 2. The equation proposed by EurOtop [1] for vertical walls and that of Franco et al. [15], give slightly higher overtopping probabilities in comparison to the theoretical curve. Surprisingly, the curve of Victor et al. [56] with $\cot\alpha$ = 0.36 (steep slope) has a P_{ow} lower than those proposed by EurOtop [1] and Franco et al. [15] for vertical walls but higher than the theoretical ones. This contradiction may be due to the differences in their approaches of formulae derivation as Victor et al. [56] used a regression model through key parameters to derive P_{ow} formula instead of using relative run-up directly (Eq. 19).In contrast to EurOtop [1] and Franco et al. [15] in which P_{ow} was conventionally related to the relative run-up, Victor et al. [56] directly investigated the effect of three parameters namely slope angle, relative crest freeboard (R_c/H_{m0}) and wave steepness on P_{ow}. Accordingly, they found that the effect of wave steepness on the probability of overtopping is negligible and provided an equation based on only $\cot\alpha$ and R_c/H_{m0} (see Appendix B for details).

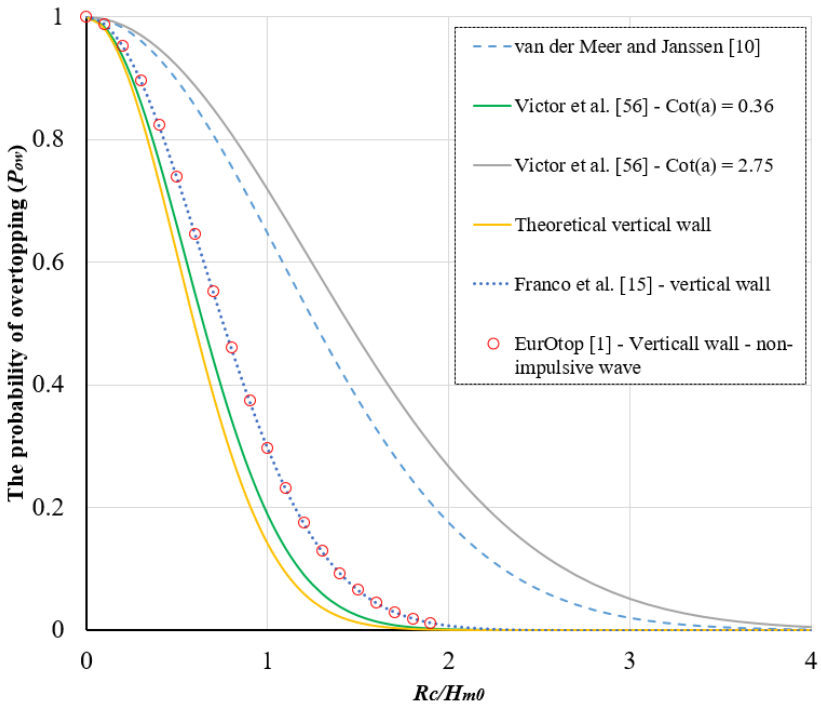

Fig. 4. Relative crest freeboard against the probability of overtopping, different studies

3. Overtopping flow thickness, velocity and discharge

In cases where the safety of people or vehicles at the crest of the structure is important, more information other than simply the volume of severe overtopping waves is required [64,65]. Even if the maximum overtopping volume is acceptable, there is no guarantee that an overtopping event with excessive flow depth (thickness) (h) or velocity (u) will not endanger people and vehicles safety. Determining safety criteria for people or vehicles requires an understanding of their failure mechanisms and the nature of the flow. The product of flow velocity (u) and thickness (h), $u.h$, is the most common parameter used to define the safety limits for different hazard regimes. For example, based on the recommendation of Ball et al. (ARR) [19], $u.h$ values less than 0.4 m^2/s and 0.6 m^2/s provide low hazards for children and adults respectively while $u.h$ > 1.2 m^2/s imposes extreme hazards for any pedestrians. Similar safety limits for vehicles based on $u.h$ values can be found in other studies e. g. [19,66] in which different instability modes such as sliding, toppling or floating have been considered. Fig. 5 demonstrates the thresholds for overtopping flow velocity and thickness on the crest of breakwater proposed [64] for the safety of pedestrians. Generally speaking, these curves imply that the product of overtopping flow thickness and velocity should be limited. Ball et al. [19] pointed out that the flow velocity and thickness should be limited to 3 m/s and 0.5 m (for children). These values are large and are likely not conservative; more detailed studies to derive accurate estimates of critical velocities, critical layer thickness, and critical volumes are needed. In the cases that the structure itself is potentially vulnerable, overtopping flow velocity plays a major role. The large forces due to the jumping of overtopping flow on the crest [67] or the surface erosion of dikes (leeward slope) due to the accelerating overtopping flow [68] are examples of the other cases in which overtopping flow velocity / thickness needs to be considered.

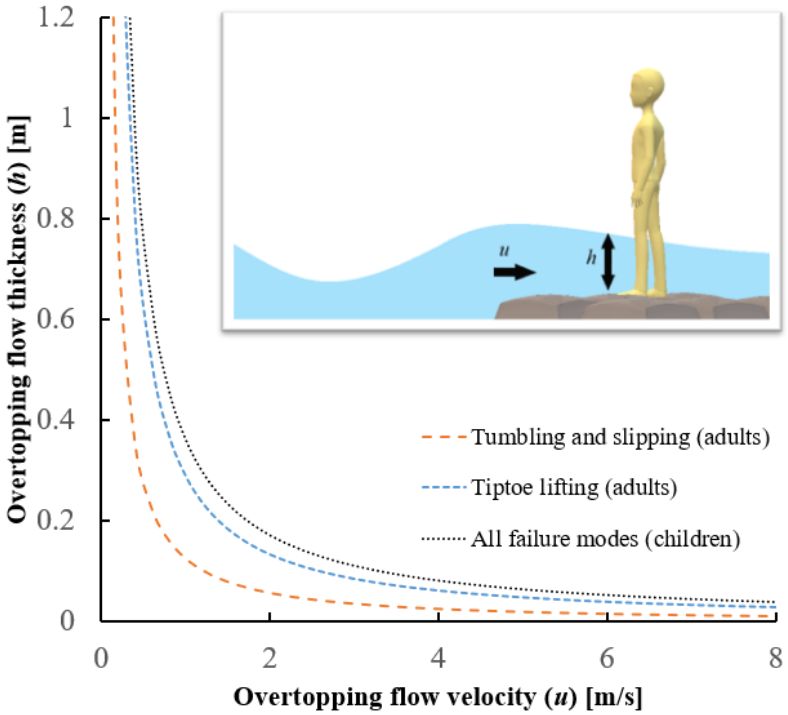

Fig. 5. Overtopping flow velocity and thickness limits for pedestrian stability given by Bae et al. [64] at the crest of breakwater

The overtopping responses (flow thickness and velocity) are temporally and spatially variable over the structure. Hence, by considering the vulnerable points or aspects of the project in terms of protection (e.g. people, vehicles) or structural stability, overtopping responses can be studies. The theoretical formula to calculate the depth of overtopping flow was first proposed by Cox and Machemehl [69] which was later modified by Wallace et al. [70] (Appendix D). Schüttrumpf and Van Gent [11] suggested that both overtopping flow thickness ($h_{2\%(x_c=0)}$) and velocity ($u_{2\%(x_c=0)}$) at the seaward edge of the crest (x_c is position on the crest with respect to its beginning) depend on the difference between 2% run-up height and freeboard crest as:

$$\frac{h_{2\%(x_c=0)}}{H_s} = c'_h \left(\frac{R_{u2\%} - R_c}{H_s}\right) \quad (20)$$

$$\frac{u_{2\%(x_c=0)}}{\sqrt{gH_s}} = c'_u \sqrt{\frac{R_{u2\%} - R_c}{H_s}} \quad (21)$$

where c'_h and c'_u are empirical coefficients which depend on the geometry of the structure. Table 2 summarizes the values of these coefficients for the seaward side of the crest obtained by different studies. The coefficient c'_h proposed by Schüttrumpf [12] is more than twice of that of Van Gent [13]. Bosman [71] analysed the data of both mentioned studies and concluded that the measured velocity values of large-scale experiments of Schüttrumpf [12] were incorrect, mainly due to high turbulent and air containing flow. Bosman [71] and Bosman et al. [72] incorporated the effect of the seaside slope of the structure and proposed $c'_h = 0.01/\sin^2\alpha$ and $c'_u = 0.3/\sin\alpha$ for dikes with $\cot\alpha$ = 3,4 and 6. Van der Meer et al. [73] conducted experiments on dikes and pointed out that the overtopping flow thickness at the seaward crest is 50% larger than the flow thickness along the crest. They considered the seaward slope effect (only on the overtopping flow velocity) and proposed $c'_u = 0.35 \cot\alpha$. EurOtop [1] recommends $c'_h = 0.2$ and $c'_h = 0.3$ for sloped structures ($\cot\alpha$ = 3,4 and 6 respectively). Based on several experimental and numerical tests on dikes ($2 \leq \cot\alpha \leq 6$), Formentin et al. [74] proposed the following power equations instead of traditional linear forms with $b_0 = 1$:

$$h_{2\%(x_c=0)} = a_h \left(R_{u2\%} - R_c\right)^{b_0} \quad (22)$$

$$u_{2\%(x_c=0)} = a_u \left(\sqrt{g(R_{u2\%} - R_c)}\right)^{b_0} \quad (23)$$

where $a_h = 0.085\cot\alpha$, $a_u = 0.12\cot\alpha + 0.41$ and $b_0 = 1.35$.

Table 2: The proposed values of coefficients c'_h and c'_u by several authors

Author(s)	c'_h	c'_u	Structure Type
Schüttrumpf [12]	0.35	1.37	Dike - $\cot\alpha$ = 3, 4
Van Gent [13]	0.15	1.33	Dike - $\cot\alpha$ = 4
Bosman [71]	$0.01/\sin^2\alpha$	$0.3/\sin\alpha$	Dike - $\cot\alpha$ = 4, 6
Van der Meer et al. [73]	-	$0.35\cot\alpha$	Dike - $\cot\alpha$ = 3, 4, 6
EurOtop [1]	$\begin{cases}0.2\\0.3\end{cases}$	-	$\begin{cases}\text{Dike} - \cot\alpha = 3,4\\ \text{Dike} - \cot\alpha = 6\end{cases}$
Mares-Nasarre et al. [22]	0.52	-	Breakwater - $\cot\alpha$ = 1.5

3.1. Overtopping variation in time (*temporal evolution*)

As discussed in the previous sections, the record of an individual overtopping event (thickness, velocity or discharge) is bell-shaped with rising and falling limbs (see Fig. 6). Zanuttigh and Martinelli [75] described the temporal evolution of an overtopping events by defining the rise time (t_r) and the duration time (t_d) parameters. Later, Formentin and Zanuttigh [23] concluded that the ratio t_r/t_d does not exceed 0.5, and is mostly between 0.15 and 0.35. They also found that t_r/t_d gradually increases as the overtopping flow evolves across the crest. In several mathematical equations proposed for the temporal variation of overtopping parameters e. g. [71,76,77], the rising limb is commonly neglected due to the short duration. Equations (24) and (25) are the power functions proposed by Hughes and Shaw [77] for overtopping flow thickness and velocity variations:

$$h\,(x_c, t) = h_{2\%(x_c)}\ \left(1 - \frac{t}{t_{ov,2\%\,(x_c)}}\right)^{b_h} \tag{24}$$

$$u\,(x_c, t) = u_{2\%(x_c)}\ \left(1 - \frac{t}{t_{ov,2\%\,(x_c)}}\right)^{b_u} \tag{25}$$

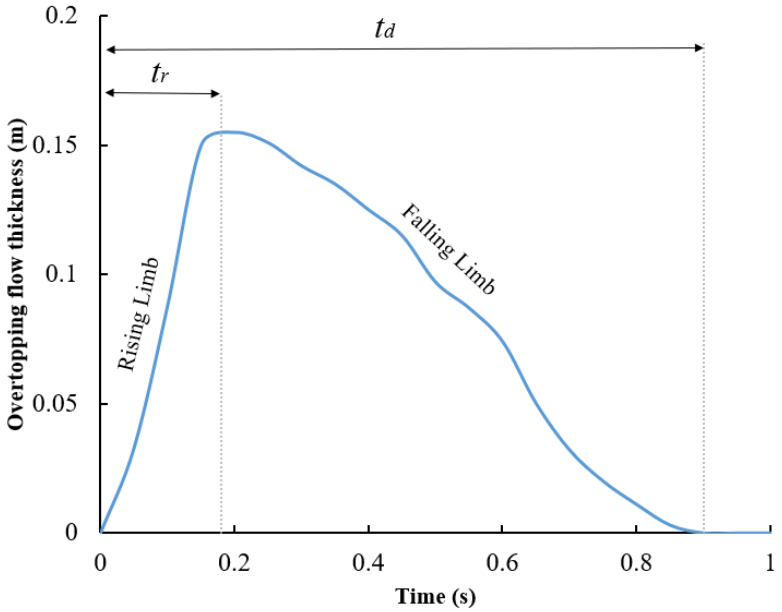

Fig. 6. Temporal variation of flow thickness during a single overtopping event (schematic)

Using the volume (V_f) and occurrence duration (t_{ov}) of a single overtopping event, its mean overtopping discharge $q_m = V_f/t_{ov}$ can be easily calculated. However, in order to visualize an overtopping event in a better way, the momentary discharge of an overtopping event $q_f(t)$ which is the product of overtopping flow thickness and velocity is used:

$$q_f(t) = h\,(t).\,u\,(t) \tag{26}$$

Fig. 7 shows the time series of given parameters in Eq. (26), for five consecutive overtopping events. Hughes et al. [61] noticed that the maximum overtopping flow thickness and maximum velocity do not occur at the same time. Hence, the occurrence times of maximum discharge, maximum thickness and maximum velocity could be different. Hughes and Thornton [49] used the following two-parameter Weibull distribution for the time variation of individual overtopping discharge on dikes:

$$q_f(t) = \frac{V_f b}{a}\left(\frac{t}{a}\right)^{b-1} exp[-\left(\frac{t}{a}\right)^{b}] \tag{27}$$

Here, the shape factor is assumed to be equal to 2 and the scale factor is a function of q_m and V_f (the total volume of a single overtopped wave). Accordingly, the theoretical $q_{max,f}$ and its occurrence time were derived as:

$$t_{max} = a\left(\frac{b-1}{b}\right)^{\frac{1}{b}} \tag{28}$$

$$q_{max,f} = \frac{V_f b}{a}\left(\frac{b-1}{b}\right)^{\frac{b-1}{b}} exp[-\left(\frac{b-1}{b}\right)] \tag{29}$$

Similar to q_m, $q_{max,f}$ for each single wave seems to be directly related to its V_f and duration of occurrence ($V_f \propto q_{max,f}.t_{ov}$). Although some studies (Appendix C) have experimentally

correlated $q_{max,f}$ to the slope of structure and the volume of individual event (V_f), no clear relationship has been suggested between $q_{max,f}$ and common wave and structural parameters. Finding the relationship between the distributions of wave overtopping volumes and the maximum momentary discharges can be the aim of future studies.

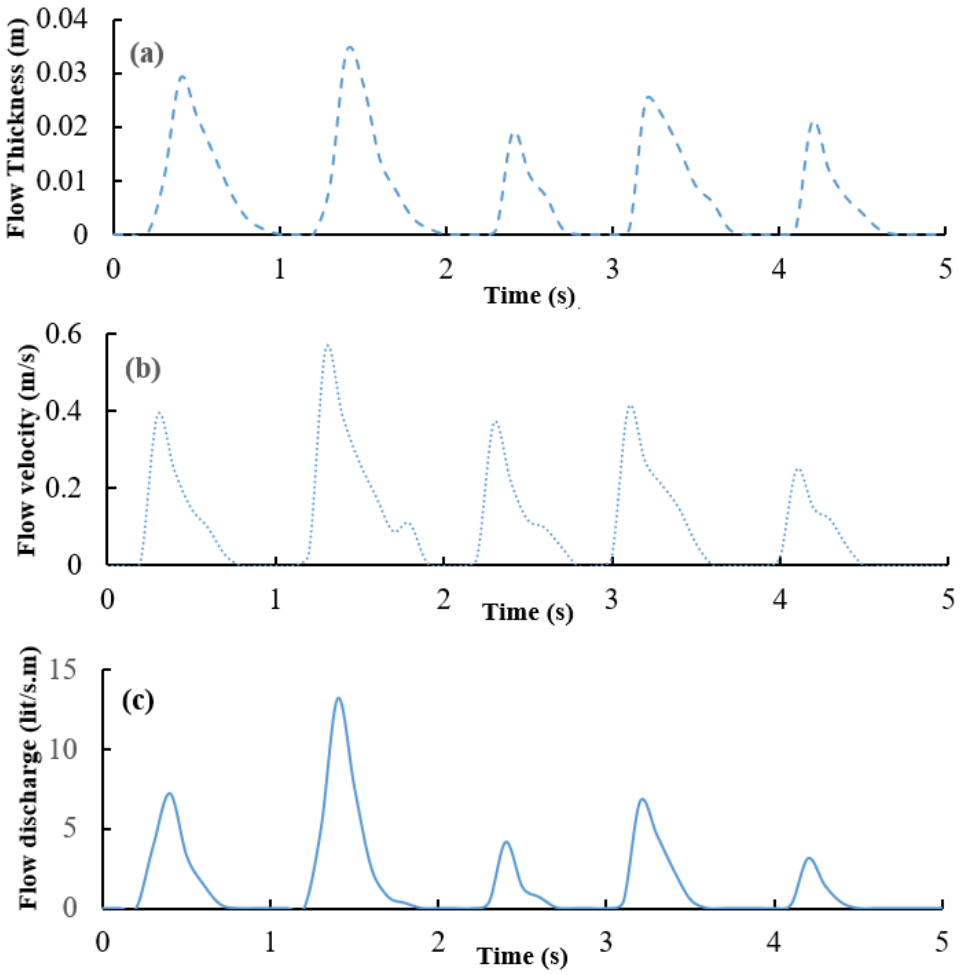

Fig. 7. Time series of (a) overtopping flow thickness, (b) velocity and (c) discharge (schematic)

3.2. Measurement techniques

The measurement of the velocity for a non-uniform and unsteady overtopping flow with rapid variations is difficult especially when the flow is turbulent and aerated at the seaward edge of the crest [12]. Besides the inherent complex nature of the overtopping, some other challenges exist in small-scale experiments (e. g. boundary effects). The simplest way to measure the overtopping velocity is by using a micro-propeller e. g.[13,22,62](Fig. 8). Despite being one of the widely used instruments, care needs to be taken to ensure that the propeller is working properly and responds instantaneously when a layer of water reaches the propeller. If there is a gap between the circular frame of the micro-propeller and the structure surface, the flows with the depth less than the gap thickness cannot be detected. However, this can be solved as for instance by embedding the propellers' frame partially where there is no gap between the

propeller and the slope [13]. Even if the probe is partially submerged, the data should be used cautiously and the flow direction should be known, especially when a backward flow may occur. Validation of the equipment is important to increase the reliability of acquired data from a micro-propeller. The micro-propeller should be calibrated for conditions where the velocity is known. For example, two micro-propellers can be installed at the structure crest with a specific distance in the direction of the flow. Based on the assumption that the overtopping event at most of the emerged structures (e. g. dikes) occurs in breaking wave conditions [78], the flow velocity (u) and the velocity of propagation of the wave front known as celerity (c) should be approximately equal [23].

Another class of velocity measurement instrument uses the Doppler effect which calculates the velocity of a moving object through the difference in the received frequency in comparison to the stationary state. Ultrasonic Doppler Velocimeter (UDV)[79], Acoustic Doppler Velocimeter (ADV)e. g. [80] and Laser Doppler Velocimeter (LDV)(e.g. [60,77]) are some examples of the Doppler effect-based instrumentations used to measure the velocity at a single point. Some other types of instrumentations based on the Doppler effect known as the profilers are able to measure the profile of the velocity along an arbitrary direction e. g. [74,81]. Although the Doppler effect-based instrumentations have higher accuracy than the mechanical ones, they have also some limitations. For example, UDVs are designed only for liquid mediums and can be used only in the submerged form. If the sensor is placed above the free surface of water or the water contains air bubbles, the detected signal will not be reliable.

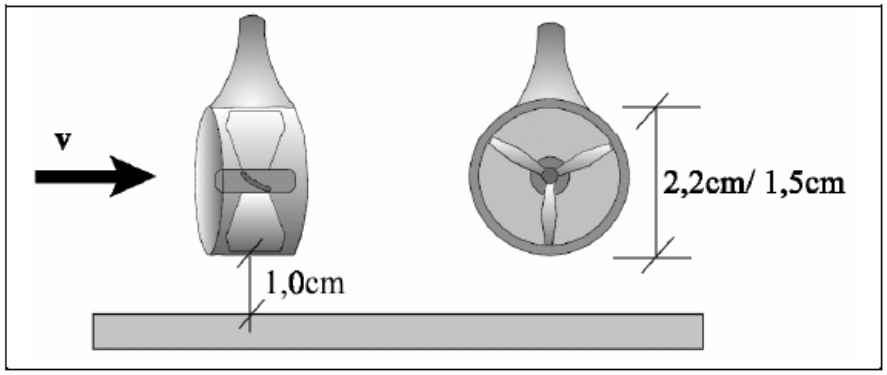

Fig. 8: Micro-propeller [82]

The third technique to measure the flow velocity is using the remote sensing approaches in which the flow movement is recorded by high-speed cameras and the captured images are processed. The calculation of velocity through image processing was initially employed in the basic study of fluid mechanics e. g. [83,84] and then developed for breaking wave conditions e. g. [85–87]. Particle Image Velocimetry (PIV) is one of the most widely used techniques of remote sensing velocimetry e. g. [88]. In PIV methods, the flow is illuminated (usually by a laser light sheet) and the velocity is measured by tracing the paths of objects which naturally exist in the flow (e. g. foam) or are seeded intentionally [89]. Chang and Liu [90] reported that when the wave breaks and entrains air bubbles, the PIV technique is restricted to only outside the aerated area and the breaking wave front is lost. Introduced by Ryu et al. [91], Bubble Image Velocimetry (BIV) is a modified version of PIV which correlates consecutive bubble images to determine their velocities. Since the BIV technique does not require illumination, its set up has a lower cost in comparison to PIV. Even though BIV is conceptually simple, there

are important details that must be considered for the application of this method to obtain reliable results. The successful application of the BIV technique for wave overtopping problem in aerated flow can be found in [92,93]. Raby et al. [93] used BIV to estimate velocity, wave overtopping discharge and hence overtopping volumes. Fig. 9 compares the performances of BIV with those of weir analogy and numerical model.

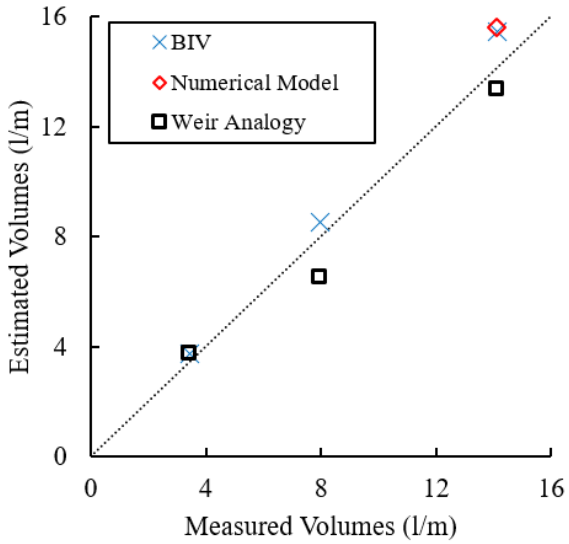

Fig. 9: Estimated overtopping volumes compared with measured overtopping volumes for steep fronted wave, after [93]

For overtopping flow depth or thickness (*h*) measurements, different techniques have been reported. Wave gauges have been widely used in overtopping experiments to measure flow depth e. g.[13]. Generally, the mechanism of the wave gauges is based on measuring the electrical resistance between two parallel wires. When flows are turbulent, perhaps due to spray, a wave gauge may record a higher flow thickness / depth than the actual values [71]. A multi-pin depth gauge is another instrument to measure flow depths in which a series of small pins are mounted at a given spacing (for example 1 *cm*) on a vertical board e. g. [12]. The flow thickness (depth) can be measured based on the number of submerged pins. The main problem of the multi-pin depth gauge is that records appear in a stepped graph in increments of the pin height. Since the depth gauge has a similar mechanism to the wave gauge as mentioned, measurement of the aerated flow thicknesses/depths may be challenging. Therefore, a video camera is usually suggested to be installed along with the wave gauge or depth gauge in order to increase the experiment's reliability. Pressure cells installed at the surface of the structure have also been used to estimate the flow thickness. Schüttrumpf [12] and Bosman [71] assumed hydrostatic pressures and showed that pressure cells miss some overtopping events or they underestimate the maximum thickness. Recently, LIDARs (Light Detection And Ranging) have successfully been used to record time-varying free-surface profiles e. g. [94,95]. A LIDAR is a laser measurement sensor that reads the free surface based on the time of flight principle. This instrument is suitable for continuous measurement of water surface profile as it can replace large arrays of conventional point-reader probes (e. g. wave gauges). Blenkinsopp et al. [94] concluded that the location of the instrument is very important and if it is positioned

appropriate for the main area of interest, the results will be reliable. The capability of LIDARs to record the free surface of turbulent and fully-aerated flow has been reported by Montano et al. [96] and Montano and Felder [97].

4. Summary and Conclusions

Wave-by-wave analysis is a step forward in the study of wave overtopping on coastal structures. The mean overtopping discharge may not give enough information in many cases and the critical conditions caused by the larger waves should be assessed. The probability distribution of individual overtopping volumes determines the probability of a single overtopping event with a certain volume based on structural and wave parameters. The temporal evolution of the characteristics of an individual overtopping event, such as thickness and velocity need to be studied as their maximum values should be considered as design criteria. At present, the amount of accurate data on wave-by-wave overtopping, and the thickness and velocities in individual overtopping events, is significantly less than for the mean overtopping discharge. As discussed, wave-by-wave studies are more time consuming and expensive as more instrumentations are required in order to measure the characteristics of a single overtopping event. Moreover, for the continuous detection of records (time series), the adoption of some techniques to remove the noise and interpret the obtained data is necessary. A summary of the main findings and the existing challenges of individual wave overtopping studies as well as some prospects for future studies are given below:

- Measurement of an individual overtopping volume:
  The volume of an individual overtopping event is one of the important parameters that needs to be measured using a container behind the structure. In general, there are three techniques to measure overtopping volumes in overtopping containers in a laboratory, using: 1) wave gauges, 2) pressure transducer, or 3) weighing systems. In this paper, the capabilities and drawbacks of the mentioned techniques were discussed. The selection of the most appropriate method depends on the project's needs and characteristics. A researcher should be aware of the existing limitations of each technique and know how to minimize the measuring errors by providing a suitable experimental design. For wave-by-wave measurements in the field, studies are very limited. As a traditional method, placing a tank at the crest of structure to collect overtopping water with a continuous draining system is the simplest way to study overtopping in wave-by-wave form. Recently, the WireWall system has been used to measure overtopping parameters as an alternative to the traditional in-situ systems using a collection tank. As yet, the capability of this technique has not been fully proven as only preliminary results from field measurements have been reported so far. The comparative assessment of Wirewall against traditional water tank systems in different conditions can be the aim of future studies.
  The results of the analysis suggest that scale effects are more significant for rubble mound structures than for vertical walls. Hence, investigating the source of the inconsistencies between small-scale and field measurements and generating field measurement data for model validation are suggested for future studies.

- Identification of an individual wave overtopping event:
  During an experiment, the occurrence of the overtopping events should be detected using continuous records. The records can be the time series of overtopping flow thickness obtained from a wave gauge installed at the crest of the structure (or inside the container) or the cumulative volume curve. Due to potential noise in the measured signals, identifying overtopping events using the cumulative volume curve is complicated, especially when a pumping system is used during an overtopping event. When using the wave gauge signal, some automatic techniques use up / down crossing. Even though the selection of an appropriate threshold for up / down crossing can improve the process, observations showed that a considerable number of (small) events are not detected, although the most important (large) volumes are likely to be captured. The wave coupling system in which at least two wave gauges are installed on the crest of structure with a certain distance in the direction of overtopping flow can efficiently increase the accuracy of the detection system because of the double-check procedure to remove noises. Besides the automatic techniques, manual (human supervised) control is highly recommended because some unpredictable conditions may lead to imprecise identification. Moreover, for future studies, it is suggested to investigate the role of very small overtopping events as their detection is difficult and expensive. In addition, the possibility of ignoring small events in the measurement and using the extrapolation of frequency histogram from the lower threshold down to the zero needs to be studied.

- Probability distribution (volume)
  The Weibull function with two adjustable parameters (shape and scale factors) is generally used to describe the distribution of individual wave overtopping volumes and estimate the maximum probable individual overtopping volume (V_{max}). In the early studies of wave overtopping Weibull shape factor (b) was considered as a constant value (e. g. $b = 0.75$). Recently, several studies were conducted to correlate the Weibull shape factor to different wave and structural parameters where the most popular ones are those considering the relative crest freeboard (R_c/H_{m0}) and the slope angle ($\cot\alpha$). Generally, structures with the negative crest freeboard (submerged) ($R_c/H_{m0} < 0$) have higher b values. For emerged structures, by increasing the relative crest freeboard the shape factor decreases until it reaches to a constant value for $R_c/H_{m0} = 1$. Structures with steep slopes (smaller $\cot\alpha$) have slightly larger b values in comparison to structures with gentle slopes. Given that most of the available results are based on 2D laboratory tests, it is not yet fully understood how 3D effects such as oblique wave and short-crested waves affect the overtopping volumes, velocities, and layer thickness. Therefore, future studies can aim to investigate how the mentioned aspects can affect the results and what can be done to improve the existing design guidelines in terms of the estimation of the critical overtopping conditions.

- Probability of overtopping
  The probability of overtopping (P_{ow}) plays an important role in the distribution of the overtopping volumes. In general, P_{ow} is related to the relative crest freeboard (R_c/H_{m0}) and the coefficient χ using an exponential function. The χ coefficient depends on the relative run-up ($R_{u2\%}/H_{m0}$) and eventually to the Iribarren number. For the structures with zero crest freeboard, P_{ow} is assumed to be unity and by increasing R_c/H_{m0}, P_{ow} reduces rapidly. For vertical walls, P_{ow} decreases sharply when R_c/H_{m0} increases so

that for R_c/H_{m0} = 2 no overtopping is likely to occur while sloped structures may experience overtopping even for R_c/H_{m0} = 4.

- Temporal variation of overtopping parameters
  The records of overtopping flow thickness / velocity show a sharp increase when the front arrives while later on the thickness / velocity more gradually reduces. A mean discharge of an individual overtopping event (q_m) can be calculated through its total volume (V_f) and the duration of occurrence (t_{ov}). In order to obtain the maximum momentary discharge of a single overtopping event ($q_{max,\ f}$), the time series of overtopping flow thickness and velocity are required. As limited studies on the relationship between $q_{max,f}$ and other wave and structural parameters are reported, future research on this topic may be useful.
  The probability distributions of individual wave parameters such as flow thickness and velocity have not been reported in the literature. Future studies can investigate the relationships between the distribution of these parameters and that of the overtopping volume. The estimation of the distribution of individual overtopping discharge and the maximum overtopping discharge based on the distribution of individual overtopping volume are also recommended to be studied for different types of structures.

- Measurement of overtopping flow velocity
  Three main used methods are: 1) mechanical (micro-propeller), 2) Doppler effect-based and 3) remote sensing ones. Using a micro-propeller is the easiest and the most in-expensive way to measure overtopping flow velocities. A micro-propeller can be used as a reliable instrument provided all mentioned practical points to be checked to ensure their correct recordings. These points include the position of the instrument on the crest, the turbulence of flow and, the submergence and the response-time of the propellers. Several instruments (e.g. UDVs, AVDs, LDVs, …) of Doppler-based approaches are used in the wave overtopping studies which can be categorized into two main groups: point readers and profilers. These instruments are generally designed for a uniform medium (liquid) and may not be appropriate for flows with a large amount of entrained air or bubbles. Remote sensing approaches are based on image processing using (high-speed) cameras where the user needs to be experienced enough to conduct all procedure including lightening (if applicable), the capturing and processing of images appropriately. As a suggestion for future studies, the accuracy of the mentioned techniques for the measurement of overtopping flow velocity can be compared.

- Measurement of overtopping flow thickness
  Overtopping flow thicknesses are usually measured by a wave gauge. A depth / step gauge can also be used on the structure crest which gives the records in a step form. One of the common problems in using these instruments is that sprays and bubbles in aerated flows (where the flow depth is read) may show more than the actual water depth. Therefore, the use of a video camera can help to detect the existence of such spray and/or bubbles. LIDARs can also be used as an alternative to the arrays of wave gauges which reads the longitudinal free surface profile of water flow.

Acknowledgements
This paper depends on the hard work in laboratory and field experiments by the many researchers who have provided the references reviewed here. The authors want to thank them (and their research funders), and acknowledge that this paper could not have been produced without those efforts. Also, the authors would like to acknowledge the financial support from Griffith University. The first author was funded by GUPRS and GUIPRS scholarships.

lossary

a: Weibull scale factor	q_1: continuous record of the derivative of the volume
a': $\Gamma(1+\frac{1}{b})$	q^*: dimensionless mean overtopping discharge defined by $q/gH_sT_{m-1,0}$
b: Weibull shape factor	$R_{u2\%}$: run-up level exceeded by the 2% of the coming waves
B: berm length	R_h: dimensionless crest freeboard defined by $R_h = (\frac{R_c}{H_s})(\frac{h_t}{H_s})\frac{2\pi h_t}{gT_m^2}$
c: wave celerity	R_c: crest freeboard
c_d: maximum wave celerity	S_f: sampling frequency
c_s: minimum possible celerity in shallow water	$s_{m-1,0}$: wave steepness defined by $2\pi H_{m0}/gT_{m-1,0}^2$
d_b: water depth on the berm	s_{op}: wave steepness defined by $2\pi H_s/gT_p^2$
dt_{min}: minimum lag between the detected events in the coupling process	T_m: mean wave period
dt_{max}: maximum lag between the detected events in the coupling process	$T_{m-1,0}$: spectral wave period
d_w: distance between two wave gauges at the crest of structure in the direction of flow	T_p: peak wave period
g: acceleration due to gravity	T: wave period to be added
H_{m0}: spectral wave height	t: time
H_s: significant wave height	t_{ov}: overtopping time
$H_{1/10}$: average of the 1/10 highest incident waves	u: flow velocity
h: flow thickness	u_{th}: lower threshold of up/down- crossing method
h_{max}: maximum overtopping flow thickness	$\bar{V}$: mean overtopping volume
h_t: water depth at the structure toe	V: overtopping volume
h^*: $\frac{h_t}{H_s}(\frac{2\pi h_t}{gT_m^2})$	V_f: volume of an individual overtopping event
h_{1min}: measured flow thickness at the first wave gauge	V_0 : accumulated overtopping volume
$L_{m-1,0}$: deep water wavelength defined by $1.56T_{m-1,0}^2$	V_{max}: maximum individual wave overtopping volume
$L_{0,p}$: deep water wavelength	$\bar{V}_{meas}$: measured mean overtopping volume
l_{th}: lower threshold of up/down- crossing method	V_T: threshold value to identify the overtopping events
N_w: number of waves	$\bar{V}_{theor}$: theoretical mean overtopping volume
N_{ow}: number of overtopping waves	x_c: position on the dike crest with respect to the beginning of the dike crest
$\hat{P}$: exceedance probability of each overtopping wave	α: angle of seaward slope of structure
P_v: exceedance probability of each overtopping volume	$\gamma_{b,sf}$: reduction factor for berm effect on shape factors
P_{ow}: probability of overtopping	$\gamma_{b,p}$: reduction factor for berm effect on probability of overtopping
q: mean overtopping discharge	γ_f: roughness factor
q_f: momentary discharge of an individual overtopping event per unit length	γ_{f-surf}: modified roughness factor
q_m: mean overtopping discharge of a single wave	γ_h: shallow foreshore factor
$q_{max,f}$: maximum momentary discharge of individual overtopping event	γ_β: oblique wave factor
q_w: overtopping discharge at submerged structures	γ_b: berm factor
q_{ws}: average discharge at submerged structures	ξ_p: Iribarren number defined by $tan\,\alpha/\sqrt{H_s/L_p}$
q_s: surge overflow discharge	$\xi_{m-1,0}$: Iribarren number defined by $tan\,\alpha/\sqrt{H_{m0}/L_{m-1,0}}$

References

[1] J.W. Van der Meer, N.W.H. Allsop, T. Bruce, J. De Rouck, A. Kortenhaus, T. Pullen, H. Schüttrumpf, P. Troch, B. Zanuttigh (*Eds*.), EurOtop, 2018. Manual on wave overtopping of sea defences and related structures. www.overtopping-manual.com.

[2] H. Shi-igai, T. Kono, Analytical approach on wave overtopping on levees, in: Proc. 12th Int. Conf. Coast. Eng., 1970: pp. 563–573.

[3] H. Shi-Igai, H. Rong-Chung, An analytical and computer study on wave overtopping, Coast. Eng. 1 (1977) 221–241.

[4] V.M. van Bergeijk, J.J. Warmink, M.R.A. van Gent, S.J.M.H. Hulscher, An analytical model of wave overtopping flow velocities on dike crests and landward slopes, Coast. Eng. 149 (2019) 28–38. https://doi.org/10.1016/j.coastaleng.2019.03.001.

[5] J. van der Meer, T. Pullen, W. Allsop, T. Bruce, H. Schüttrumpf, A. Kortenhaus, Prediction of overtopping, Handb. Coast. Ocean Eng. Expand. Ed. 1–2 (2017) 563–604. https://doi.org/10.1142/9789813204027_0021.

[6] US Army Corps of Engineers. Coastal engineering manual, Eng. Man. 1110--2-1100. (2002).

[7] TAW, Technical report wave run-up and wave overtopping at dikes, Tech. Advis. Comm. Flood Defence, Delft, Netherlands. (2000).

[8] G. J. Steendam, J.W. van der Meer, H. H. Verhaeghe, P. Besley, L. Franco, M.R.A. Van Gent, The international database on wave overtopping, in: Proc. 29th ICCE 4, 4301-4313, World Scientific, 2004: pp. 4301–4313.

[9] J. de Rouck, J. Geeraerts, CLASH-Crest level assessment of coastal structures by full scale monitoring, neural network prediction and hazard analysis on permissible wave overtopping.final report: full scientific and technical report, 2005.

[10] J.W. van der Meer, J. Janssen, Wave run-up and wave overtopping at dikes and Revetments, Delft Hydraulics, publication no. 485, VdM VML EB MT2. (1994).

[11] H. Schüttrumpf, M.R.A. van Gent, Wave overtopping at seadikes, Coast. Struct. 2003 - Proc. Conf. 40733 (2003) 431–443. https://doi.org/10.1061/40733(147)36.

[12] H. Schüttrumpf, Wellenüberlaufströmung an Seedeichen: Experimentelle und theoretische Untersuchungen, PhD Thesis, Technical University of Braunschweig, 2001.

[13] M.R.A. van Gent, Low-exceedance wave overtopping events: Measurements of velocities and the thickness of water-layers on the crest and inner slope of dikes, Delft Cluster, 2002.

[14] C. Franco, L. Franco, Overtopping formulas for caisson breakwaters with nonbreaking 3D waves, J. Waterw. Port, Coastal, Ocean Eng. 125 (1999) 98–108.

[15] L. Franco, M. de Gerloni, J.W. van der Meer, Wave overtopping on vertical and composite breakwaters, in: Proc. 24th Int. Conf. Coast. Eng., 1995: pp. 1030–1044. https://doi.org/10.1061/9780784400890.076.

[16] S.R. Abt, R.J. Wittier, A. Taylor, D.J. Love, Human Stability In A High Flood Hazard Zone 1, JAWRA J. Am. Water Resour. Assoc. 25 (1989) 881–890.

[17] S.N. Jonkman, E. Penning-Rowsell, Human Instability in Flood Flows 1, JAWRA J. Am. Water Resour. Assoc. 44 (2008) 1208–1218.

[18] J. Xia, R.A. Falconer, Y. Wang, X. Xiao, New criterion for the stability of a human body in floodwaters, J. Hydraul. Res. 52 (2014) 93–104.

[19] J.E. Ball, M.K. Babister, R. Nathan, P.E. Weinmann, W. Weeks, M. Retallick, I. Testoni, Australian Rainfall and Runoff-A guide to flood estimation, Commonwealth of Australia, 2019.

[20] QUDM, Queensland Urban Drainage Manual, Queensl. Dep. Energy Water Supply. (2013) 459.

[21] J. Molines, M.P. Herrera, M.E. Gómez-Martín, J.R. Medina, Distribution of individual wave overtopping volumes on mound breakwaters, Coast. Eng. 149 (2019) 15–27. https://doi.org/10.1016/j.coastaleng.2019.03.006.

[22] P. Mares-Nasarre, G. Argente, M.E. Gómez-Martín, J.R. Medina, Overtopping layer thickness and overtopping flow velocity on mound breakwaters, Coast. Eng. 154 (2019) 103561. https://doi.org/10.1016/j.coastaleng.2019.103561.

[23] S.M. Formentin, B. Zanuttigh, Semi-automatic detection of the overtopping waves and reconstruction of the overtopping flow characteristics at coastal structures, Coast. Eng. 152 (2019) 103533. https://doi.org/10.1016/j.coastaleng.2019.103533.

[24] H.-P. Chen, M.B. Mehrabani, Lifetime wave overtopping risk analysis of sea defences subjected to changing operational conditions, Eng. Fail. Anal. 97 (2019) 464–479.

[25] R. Hui, E. Jachens, J. Lund, Risk-based planning analysis for a single levee, Water Resour. Res. 52 (2016) 2513–2528.

[26] D. Gallach-Sánchez, Experimental Study of Wave Overtopping Performance of Steep Low-Crested Structures, PhD Thesis, Ghent University, 2018.

[27] T. Lykke Andersen, H.F. Burcharth, F.X. Gironella, Single Wave Overtopping Volumes And Their Travel Distance For Rubble Mound Breakwaters, in: Coastal Structures, 2009: pp. 1241–1252. https://doi.org/10.1142/9789814282024_0109.

[28] J.P. Kofoed, Wave Overtopping of Marine Structures: utilization of wave energy, PhD Thesis, Aalborg University, 2002.

[29] J. Tedd, J.P. Kofoed, Measurements of overtopping flow time series on the Wave Dragon, wave energy converter, Renew. Energy. 34 (2009) 711–717.

[30] P. Troch, J. Geeraerts, B. de Walle, J. de Rouck, L. van Damme, W. Allsop, L. Franco, Full-scale wave-overtopping measurements on the Zeebrugge rubble mound breakwater, Coast. Eng. 51 (2004) 609–628.

[31] H.E. Williams, R. Briganti, A. Romano, N. Dodd, Experimental Analysis of Wave Overtopping: A New Small Scale Laboratory Dataset for the Assessment of Uncertainty for Smooth Sloped and Vertical Coastal Structures, J. Mar. Sci. Eng. 7 (2019) 217. https://doi.org/10.3390/jmse7070217.

[32] L. Victor, P. Troch, Development of a test set-up to measure large wave-by-wave overtopping masses, in: Proc. 3rd Int. Conf. Appl. Phys. Model. to Port Coast. Prot., 2010: pp. 1–9.

[33] M. Salauddin, J.M. Pearson, Wave overtopping and toe scouring at a plain vertical seawall with shingle foreshore: A physical model study, Ocean Eng. 171 (2019) 286–299. https://doi.org/10.1016/j.oceaneng.2018.11.011.

[34] E. Jafari, A. Etemad-Shahidi, Derivation of a new model for prediction of wave overtopping at rubble mound structures, J. Waterw. Port, Coast. Ocean Eng. 138 (2011) 42–52. https://doi.org/10.1061/(ASCE)WW.1943-5460.0000099.

[35] M.R.A. van Gent, H.F.P. van den Boogaard, B. Pozueta, J.R. Medina, Neural network modelling of wave overtopping at coastal structures, Coast. Eng. 54 (2007) 586–593.

[36] P. Troch, J. Mollaert, S. Peelman, L. Victor, J. van der Meer, D. Gallach-Sánchez, A. Kortenhaus, Experimental study of overtopping performance for the cases of very steep slopes and vertical walls with very small freeboards, Coast. Eng. Proc. 1 (2014) 2.

[37] L. Victor, Optimization of the hydrodynamic performance of overtopping wave energy converters: experimental study of optimal geometry and probability distribution of overtopping volumes, PhD Thesis, Ghent University, 2012.

[38] H. Oumeraci, Strengths and limitations of physical Modelling in coastal Engineering--synergy effect with numerical modelling and field measurement, in: Proc. HYDRALAB-Workshop Hann. Ger., 1999: pp. 7–38.

[39] A. Kortenhaus, H. Oumeraci, J. Geeraerts, J. De Rouck, J. MEDINA, J. GONZÁLEZ-ESCRIVÁ, Laboratory effects and other uncertainties in wave overtopping measurements, in: B. Abstr. 29th Int. Conf. Coast. Eng., 2004: p. 343.

[40] J. De Rouck, J. Geeraerts, P. Troch, A. Kortenhaus, T. Pullen, L. Franco, New results on scale effects for wave overtopping at coastal structures, in: Int. Conf. Coastlines, Struct. Break. 2005, 2005: pp. 29–43.

[41] T. Pullen, W. Allsop, T. Bruce, J. Geeraerts, Violent wave overtopping: CLASH field measurements at Samphire Hoe, in: Coast. Struct. 2003, 2004: pp. 469–480.

[42] J. De Rouck, B. de Walle, J. Geeraerts, P. Troch, L. Van Damme, A. Kortenhaus, J. Medina, Full scale wave overtopping measurements, in: Coast. Struct. 2003, 2004: pp. 494–506.

[43] L. Franco, G. Bellotti, R. Briganti, J. De Rouck, J. Geeraerts, Full scale measurements of wave overtopping at Ostia yacht harbour breakwater, in: Proc. Conf. Coast. Struct., 2003.

[44] R. Briganti, G. Bellotti, L. Franco, J. De Rouck, J. Geeraerts, Field measurements of wave overtopping at the rubble mound breakwater of Rome--Ostia yacht harbour, Coast. Eng. 52 (2005) 1155–1174.

[45] T. Pullen, E. Silva, J. Brown, M. Yelland, R. Pascal, R. Pinnell, C. Cardwell, D. Jones, WireWall--laboratory and field measurements of wave overtopping, in: Bundesanstalt für Wasserbau, 2019.

[46] J. Brown, M. Yelland, R. Pascal, T. Pullen, P. Bell, C. Cardwell, D.S. Jones, N. Milliken, T. Prime, G. Shannon, others, WireWall: a new approach to coastal wave hazard monitoring, in: 3 Rd Int. Conf. Prot. against Overtopping, 2018.

[47] P. Besley, Wave overtopping of seawalls, design and assessment manual, R&D technical report W178D, HR Wallingford, 1999.

[48] T. Pullen, W. Allsop, T. Bruce, J. Pearson, Field and laboratory measurements of mean overtopping discharges and spatial distributions at vertical seawalls, Coast. Eng. 56 (2009) 121–140.

[49] S.A. Hughes, C.I. Thornton, Estimation of time-varying discharge and cumulative volume in individual overtopping waves, Coast. Eng. 117 (2016) 191–204. https://doi.org/10.1016/j.coastaleng.2016.08.006.

[50] J. Platteeuw, Analysis of individual wave overtopping volumes for steep low crested coastal structures in deep water conditions, PhD Thesis, Ghent University, 2015.

[51] J.C. Su, C.I. Liu, C.T. Kuo, Application of Weibull distribution for irregular wave overtopping, in: Proc. 6th IAHR Symp. Stoch. Hyd., Taipei, Taiwan, 1992.

[52] Y. Goda, Random Seas and Design of Maritime Structures, Adv. Ser, Ocean Eng. 15 (2000) 443.

[53] B. Zanuttigh, J. van der Meer, T. Bruce, S. Hughes, Statistical characterisation of extreme overtopping wave volumes, Coasts, Mar. Struct. Break. 2013 From Sea to Shore - Meet. Challenges Sea. 1 (2013) 442–451. https://doi.org/10.1680/fsts.59757.0442.

[54] C. Franco, Wave overtopping and loads on caisson breakwaters under threedimensional sea-states, Delft Hydraul. Full Final Report. (1996).

[55] T. Bruce, J.W. van der Meer, L. Franco, J.M. Pearson, Overtopping performance of different armour units for rubble mound breakwaters, Coast. Eng. 56 (2009) 166–179.

[56] L. Victor, J.W. van der Meer, P. Troch, Probability distribution of individual wave overtopping volumes for smooth impermeable steep slopes with low crest freeboards, Coast. Eng. 64 (2012) 87–101. https://doi.org/10.1016/j.coastaleng.2012.01.003.

[57] P. Mares-Nasarre, J. Molines, M.E. Gómez-Martin, J.R. Medina, Individual wave overtopping volumes on mound breakwaters in breaking wave conditions and gentle sea bottoms, Coast. Eng. (2020) 103703.

[58] J.Q.H. Nørgaard, T.L. Andersen, H.F. Burcharth, G.J. Steendam, Analysis of overtopping flow on sea dikes in oblique and short-crested waves, Coast. Eng. 76 (2013) 43–54.

[59] Y. Pan, C.P. Kuang, L. Li, F. Amini, Full-scale laboratory study on distribution of individual wave overtopping volumes over a levee under negative freeboard, Coast. Eng. 97 (2015) 11–20.

[60] S.A. Hughes, N.C. Nadal, Laboratory study of combined wave overtopping and storm surge overflow of a levee, Coast. Eng. 56 (2009) 244–259. https://doi.org/10.1016/j.coastaleng.2008.09.005.

[61] S. Hughes, C. Thornton, J. van der Meer, B. Scholl, Improvements in describing wave overtopping processes, Proc. Coast. Eng. Conf. (2012) 1–15. https://doi.org/10.9753/icce.v33.waves.35.

[62] J.Q.H. Nørgaard, T. Lykke Andersen, H.F. Burcharth, Distribution of individual wave overtopping volumes in shallow water wave conditions, Coast. Eng. 83 (2014) 15–23. https://doi.org/10.1016/j.coastaleng.2013.09.003.

[63] Q. Ju, S. Liu, W. Huang, G. Zhong, Berm Effects on the Probability Distribution of

Individual Wave Overtopping Discharge over a Low-Crested Sea Dike, J. Waterw. Port, Coastal, Ocean Eng. 145 (2019) 04019012. https://doi.org/10.1061/(asce)ww.1943-5460.0000507.

[64] H.U. Bae, J.Y. Yoon, K.M. Yun, N.H. Lim, Human Stability with respect to Overtopping Flow on the Breakwater, Int. J. Appl. Eng. Res. 11 (2016) 111–119.

[65] C. Sandoval, T. Bruce, Wave overtopping hazard to pedestrians: video evidence from real accidents, in: Coasts, Mar. Struct. Break. 2017 Realis. Potential, ICE Publishing, 2017: pp. 501–512.

[66] G.P. Smith, B.D. Modra, S. Felder, Full-scale testing of stability curves for vehicles in flood waters, J. Flood Risk Manag. 12 (2019) e12527.

[67] X. Guo, B. Wang, H. Liu, G. Miao, Numerical simulation of two-dimensional regular wave overtopping flows over the crest of a trapezoidal smooth impermeable sea dike, J. Waterw. Port, Coastal, Ocean Eng. 140 (2013) 4014006.

[68] J.W. van der Meer, P. Bernardini, W. Snijders, E. Regeling, The wave overtopping simulator, Proc. Coast. Eng. Conf. (2007) 4654–4666. https://doi.org/10.1142/9789812709554_0390.

[69] J.C. Cox, J. Machemehl, Overload bore propagation due to an overtopping wave, J. Waterw. Port, Coastal, Ocean Eng. 112 (1986) 161–163.

[70] S.C. E. Wallace, R. MacArthur, Final Draft Guidelines for Coastal Flood Hazard Analysis and Mapping for the Pacific Coast of the United States. Federal Emergency Management Agency (FEMA)., 2005.

[71] G. Bosman, Velocity and flow depth variations during wave overtopping, Master Thesis, TU Delft, 2007.

[72] G. Bosman, J. van der Meer, G. Hoffmans, H. Schüttrumpf, H.J. Verhagen, Individual overtopping events at dikes, in: Coast. Eng. 2008 (In 5 Vol., World Scientific, 2009: pp. 2944–2956.

[73] J.W. van der Meer, B. Hardeman, G.-J. Steendam, H. Schüttrumpf, H. Verheij, Flow Depth And Flow Velocity Distribution of Overtopping Wave Volumes, Coast. Eng. (2010).

[74] S.M. Formentin, M.G. Gaeta, G. Palma, B. Zanuttigh, M. Guerrero, Flow Depths and Velocities across a Smooth Dike Crest, Water. 11 (2019) 2197.

[75] B. Zanuttigh, L. Martinelli, Transmission of wave energy at permeable low crested structures, Coast. Eng. 55 (2008) 1135–1147.

[76] W. van den Bos, Erosiebestendigheid van grasbekleding tijdens golfoverslag, Master Thesis, TU Delft, 2006.

[77] S.A. Hughes, J.M. Shaw, Continuity of instantaneous wave overtopping discharge with application to stream power concepts, J. Waterw. Port, Coast. Ocean Eng. 137 (2011) 12–25. https://doi.org/10.1061/(ASCE)WW.1943-5460.0000057.

[78] I.J. Losada, J.L. Lara, E.D. Christensen, N. Garcia, Modelling of velocity and turbulence fields around and within low-crested rubble-mound breakwaters, Coast. Eng. 52 (2005) 887–913.

[79] Y. Takeda, Ultrasonic Doppler velocity profiler for fluid flow, Springer Science & Business Media, 2012.

[80] S. Lorke, A. Bornschein, H. Schüttrumpf, R. Pohl, Influence of wind and current on wave-run up and wave overtopping, Hydralab IV report for KfKI, 2009.

[81] B. Zanuttigh, S.M. Formentin, G. Palma, M.G. Gaeta, M. Guerrero, J.W. van der Meer, K. Van Doorslaer, Reduction Of The Wave Overtopping Discharge At Dikes In Presence Of Crown Walls With Bull Noses, Coast. Eng. Proc. 1 (2018) 2.

[82] H.F.R. Schüttrumpf, H. Oumeraci, J. Möller, M. Kudella, Loading of the inner slope of seadikes by wave overtopping, Leichtweiss Institut für Wasserbau & Technical University Braunschweig, 2001.

[83] R.J. Adrian, Particle-imaging techniques for experimental fluid mechanics, Annu. Rev. Fluid Mech. 23 (1991) 261–304.

[84] C.E. Willert, M. Gharib, Digital particle image velocimetry, Exp. Fluids. 10 (1991) 181–193.

[85] C.A. Greated, N. Emarat, Optical studies of wave kinematics, in: Adv. Coast. Ocean Eng., World Scientific, 2000: pp. 185–223.

[86] M. Perlin, J. He, L.P. Bernal, An experimental study of deep water plunging breakers, Phys. Fluids. 8 (1996) 2365–2374.

[87] F.C.K. Ting, J.T. Kirby, Dynamics of surf-zone turbulence in a strong plunging breaker, Coast. Eng. 24 (1995) 177–204.

[88] R. Lindken, W. Merzkirch, A novel PIV technique for measurements in multiphase flows and its application to two-phase bubbly flows. 4th Int, in: Symp. Part. Image Velocim. Göttingen, Ger. Sep, 2001: pp. 17–19.

[89] A.A. Bradley, A. Kruger, E.A. Meselhe, M.V.I. Muste, Flow measurement in streams using video imagery, Water Resour. Res. 38 (2002) 51.

[90] K.-A. Chang, P.L.-F. Liu, Velocity, acceleration and vorticity under a breaking wave, Phys. Fluids. 10 (1998) 327–329.

[91] Y. Ryu, K.A. Chang, H.J. Lim, Use of bubble image velocimetry for measurement of plunging wave impinging on structure and associated greenwater, Meas. Sci. Technol. 16 (2005) 1945–1953. https://doi.org/10.1088/0957-0233/16/10/009.

[92] R. Jayaratne, A. Hunt-Raby, G. Bullock, H. Bredmose, Individual violent overtopping events: new insights, in: Int. Conf. Coast. Eng., World Scientific, 2009: pp. 2983–2995.

[93] A. Raby, R. Jayaratne, H. Bredmose, G. Bullock, Individual violent wave-overtopping events: behaviour and estimation, J. Hydraul. Res. 1686 (2019). https://doi.org/10.1080/00221686.2018.1555549.

[94] C.E. Blenkinsopp, I.L. Turner, M.J. Allis, W.L. Peirson, L.E. Garden, Application of LiDAR technology for measurement of time-varying free-surface profiles in a laboratory wave flume, Coast. Eng. 68 (2012) 1–5. https://doi.org/10.1016/j.coastaleng.2012.04.006.

[95] B. Hofland, E. Diamantidou, P. van Steeg, P. Meys, Wave runup and wave overtopping measurements using a laser scanner, Coast. Eng. 106 (2015) 20–29.

https://doi.org/10.1016/j.coastaleng.2015.09.003.

[96] L. Montano, R. Li, S. Felder, Continuous measurements of time-varying free-surface profiles in aerated hydraulic jumps with a LIDAR, Exp. Therm. Fluid Sci. 93 (2018) 379–397.

[97] L. Montano, S. Felder, LIDAR measurements of free-surface profiles and turbulent scales in a hydraulic jump, 7th IAHR International Symposium on Hydraulic Structures, Aachen, Germany, in: 2018.

[98] M.W. Owen, Overtopping of sea defences, in: Int. Conf. Hydraul. Model. Civ. Eng. Struct. Coventry, 1982.

[99] S. Lorke, A. Brüning, J. van der Meer, H. Schüttrumpf, A. Bornschein, S. Gilli, R. Pohl, M. Spano, J. Říha, S. Werk, F. Schlütter, On the effect of current on wave run-up and wave overtopping, Proc. Coast. Eng. Conf. (2010) 1–15. https://doi.org/10.9753/icce.v32.structures.13.

Appendix A. Weibull shape and scale factors

Author	Weibull parameters	Equation
Besley [47]	$b = \begin{cases} \text{non} - \text{impulsive condition } (h^* > 0.3): & \begin{cases} 0.66 & s_{op} = 0.02 \\ 0.82 & s_{op} = 0.04 \end{cases} \\ \text{impulsive condition } (h^* \leq 0.3): & 0.85 \end{cases}$	A. 1
Besley [47]	$b = \begin{cases} 0.76 & s_{op} = 0.02 \\ 0.92 & s_{op} = 0.04 \end{cases}$	A. 2
Hughes and Nadal [60]	$a = 0.79\, q_{ws} T_p$ $b = 15.7 \left(\frac{q_s}{g H_{m0} T_p}\right)^{0.35} - 2.3 \left(\frac{q_s}{\sqrt{g H_{m0}{}^3}}\right)^{0.79}$	A. 3
Hughes et al. [61]	$b = [exp(-0.6\, \frac{Rc}{H_{m0}})]^{1.8} + 0.64$	A. 4
Zanuttigh et al. [53]	$b = 0.85 + 1500 \left(\frac{q}{g H_{m0} T_{m-1,0}}\right)^{1.3}$	A. 5
Zanuttigh et al. [53]	$b = 0.73 + 55 \left(\frac{q}{g H_{m0} T_{m-1,0}}\right)^{0.8}$	A. 6
Pan et al. [59] (Large-scale)	$a = 1.017\, q_{ws} T_{m-1,0}$ $b = \begin{cases} 73.55 \left(\frac{q_{ws}}{g H_{m0} T_p}\right)^{0.76} & \frac{Rc}{H_{m0}} \leq -0.3 \\ 54.58 \left(\frac{q_{ws}}{g H_{m0} T_p}\right)^{0.63} & -0.3 < \frac{Rc}{H_{m0}} < 0 \end{cases}$	A. 7
Molines et al. [21]	$b = 0.63 + 1.25\, exp\,((-3\times 10^5)\, q^*)$ $a' = 1.4 - 0.4 \left(\frac{1}{b}\right)$	A. 8
Mares- Nasarre et al. [57]	$b = 0.8 + exp\,((-2\times 10^5)\, q^*)$ $a' = 1.5 - 0.4 \left(\frac{1}{b}\right)$	A. 9
Ju et al. [63]	$b = [exp(-0.49\, \frac{Rc}{H_{m0}})\gamma_{b,sf}]^{1.8} + 0.64$ $\gamma_{b,sf} = exp\,(-2.1 \frac{B}{L_{m-1,0}} + 0.07 \frac{d_b}{H_{m0}})$	A. 10

Appendix B. Probability of overtopping

Author	$\frac{R_{u2\%}}{H_{m0}}$	P_{ow}	Structure type
Van der Meer and Janssen [10]	$1.5\,\gamma_h\gamma_f\gamma_\beta\gamma_b\xi_p$ with the maximum of $3\,\gamma_h\gamma_f\gamma_\beta$	$exp\,(-(\frac{1}{\chi}\frac{R_c}{H_{m0}})^2)$	sloped
Owen[98]	-	$exp\,(K_1(\frac{1}{\gamma_f}\frac{R_c}{T_m\sqrt{gH_s}})^2)$ $K_1 = \begin{cases} 63.8 & \cot\alpha = 1 \\ 37.8 & \cot\alpha = 2 \\ 110.5 & \cot\alpha = 4 \end{cases}$	smoothed slopes with $1 \le cot\,\alpha \le 4$ and armoured slopes with $1 \le cot\,\alpha \le 2$
Besley [47]	-	$\begin{cases} 55.4\,q_*^{0.634} & 0 < q_* < 8\times10^{-4} \\ 2.5\,q_*^{0.199} & 8\times10^{-4} \le q_* < 10^{-2} \\ 1 & 10^{-2} \le q_* \end{cases}$	sloped $0.05 < \frac{R_c}{T_m\sqrt{gH_s}} < 0.3$
TAW [7]	$1.65\,\gamma_h\gamma_f\gamma_\beta\gamma_b\xi_{m-1,0}$ with the maximum of $\gamma_h\gamma_b\gamma_\beta\,(4 - \frac{1.5}{\sqrt{\xi_{m-1,0}}})$	$exp\,(-(\frac{1}{\chi}\frac{R_c}{H_{m0}})^2)$	sloped $0.5 < \gamma_b\xi_{m-1,0} < 8$ to 10
Victor et al. [56]	$\frac{1}{0.71-0.15\,cot\,\alpha}$	$exp\,[-((1.4 - 0.3\,cot\,\alpha)\frac{R_c}{H_{m0}})^2]$	steep low crest slopes $0.36 \le cot\,\alpha \le 2.75$
Nørgaard et al. [62]	-	$K_2\ exp\,(K_1(\frac{1}{\gamma_f}\frac{R_c}{T_m\sqrt{gH_s}})^2)$ K_1 = proposed by Owen [98] $K_2 = \begin{cases} 1 & \frac{H_{m0}}{h_t} \le 0.2 \quad \text{or} \quad H_{m0}/H_{\frac{1}{10}} \le 0.848 \\ -6.65 + 9.02\,H_{m0}/H_{\frac{1}{10}} & \frac{H_{m0}}{h_t} > 0.2 \quad and \quad H_{m0}/H_{\frac{1}{10}} > 0.848 \end{cases}$	sloped $cot\,\alpha$ =1.5
EurOtop [1]	$1.65\,\gamma_h\gamma_{f\_surf}\gamma_\beta\gamma_b\xi_{m-1,0}$ smooth: $\gamma_{f-surf} = \gamma_f$ rubble mound: $\gamma_{f-surf} = \gamma_f + (\xi_{m-1,0} - 1.8)\,(1-\gamma_f)\frac{1}{8.2}$	$exp\,(-(\frac{1}{\chi}\frac{R_c}{H_{m0}})^2)$	sloped
Mares – Nasarre [57]	-	$exp\,(-\frac{0.1}{q^{*0.3}})$	Sloped (breakwater)
Ju et al. [63]	-	$exp\,(-0.56(\frac{R_c}{H_{m0}}\frac{1}{\gamma_{b,p}})^2)$ $\gamma_{b,p} = exp\,(-4\frac{B}{L_{m-1,0}} + 0.02\frac{d_b}{H_{m0}})$	Sea dikes with berm
Theoretical	1.4	$exp\,(-(1.4\frac{R_c}{H_{m0}})^2)$	vertical walls

Franco et al. [15] (Large-scale)	1.78	exp (-$(1.1\frac{R_c}{H_{m0}})^2$)	vertical walls
Besley [47]	-	non-impulsive condition ($h^* > 0.3$): $exp\ (-\left(1.098\frac{R_c}{H_{m0}}\right)^2)$ impulsive condition ($h^* < 0.3$): $0.031R_h^{-0.99}$	vertical wall $0.03 < \frac{R_c}{H_s} < 3.2$
EurOtop [1]	-	non − impulsive condition: $exp\ (-1.21(\frac{R_c}{H_{m0}})^2)$ impulsive condition: $0.024\left[\frac{h_t^2}{H_{m0}L_{m-1,0}}\frac{R_c}{H_{m0}}\right]$ with the minimum of non − impulsive equation	vertical wall

Appendix C. Empirical equations proposed by Hughes and Thornton [49] **using the data set of Lorke et al.** [80,99]**:**

$$q_m = 0.066 \sqrt{g}\, V_f{}^{3/4} \quad \text{(C.1)}$$

$$t_{max} = \frac{1.73\, V_f{}^{1/4}}{\sqrt{g\, tan\alpha}} \quad \text{(C.2)}$$

$$q_{max} = 0.352 V_f{}^{3/4} \sqrt{g\, tan\alpha} \quad \text{(C.3)}$$

Appendix D. Theoretical formula for the calculation of overtopping flow thickness over the crest ([69,70]**):**

$$d\,(x_c) = \left[\sqrt{R_u - R_c} - \frac{5x_c}{A(1-2m)\sqrt{gT^2}}\right]^2 \quad \text{(D.1)}$$

$d\,(x_c)$: Overtopping flow thickness on the crest

R_u: Run-up

A: Inland slope factor

m: positive upward inland slope

T: wave period